AD-A122 166 IMPACT-INITIATED DAMAGE IN LAMINATED COMPOSITES(U) 1/2
NORTH CAROLINA AGRICULTURAL AND TECHNICAL STATE UNIV
GREENSBO... V S AVVA 30 SEP 82 AFOSR-TR-82-1038
UNCLASSIFIED F49620-80-C-0050 F/G 11/4 NL

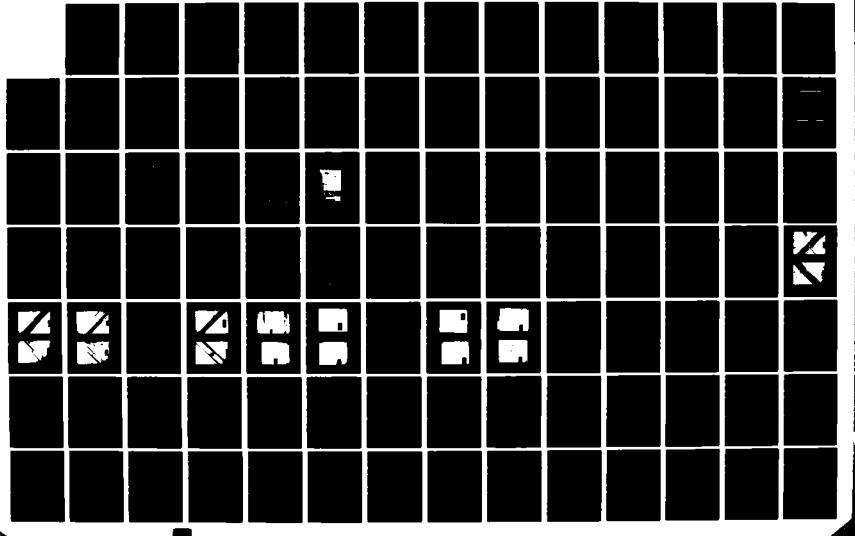

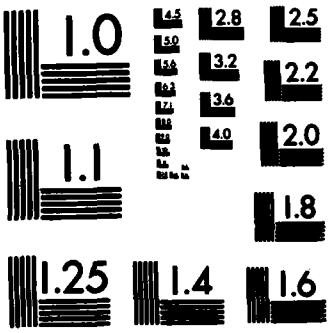

AFOSR-TR- 82-1038

NORTH CAROLINA

A & T STATE UNIVERSITY

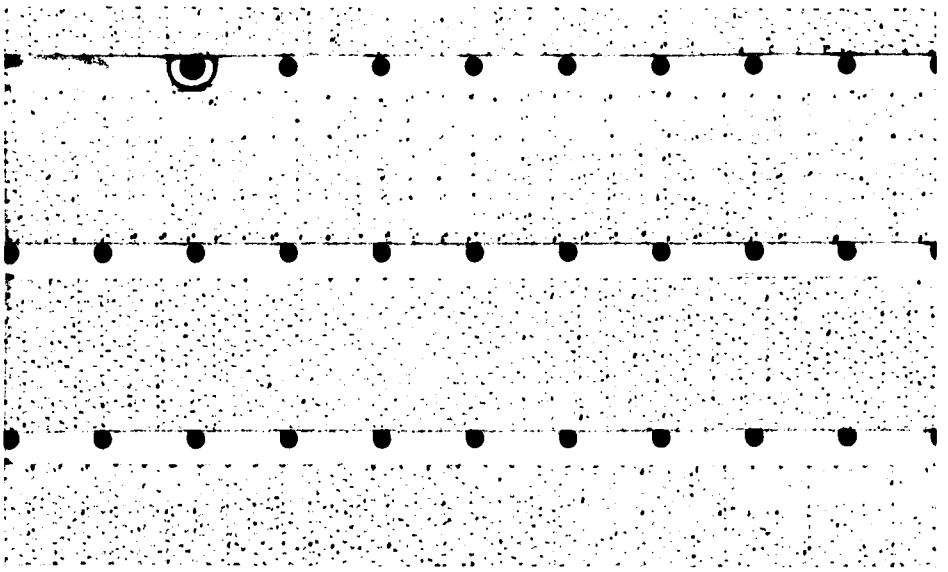

SCHOOL OF ENGINEERING

DEPARTMENT OF MECHANICAL ENGINEERING

GREENSBORO, N.C. 27411

7

FINAL REPORT

IMPACT INITIATED DAMAGE IN LAMINATED COMPOSITES

V. Sarma Avva
Professor of Mechanical Engineering

Prepared for
Air Force Office of Scientific Research
Department of Air Force
Bolling AFB, Washington, D.C.
Program Manager: Dr. Donald R. Ulrich

School of Engineering
North Carolina A&T State University
Greensboro, North Carolina

30 September, 1982

Unclassified

SECURITY CLASSIFICATION OF THIS PAGE (When Data Entered)

REPORT DOCUMENTATION PAGE	READ INSTRUCTIONS BEFORE COMPLETING FORM
1. REPORT NUMBER AFOSR-TR- 82-1038	2. GOVT ACCESSION NO. AD-A122166
	3. RECIPIENT'S CATALOG NUMBER
4. TITLE (and Subtitle) Impact-Initiated Damage in Laminated Composites	5. TYPE OF REPORT & PERIOD COVERED Final Report
	6. PERFORMING ORG. REPORT NUMBER
7. AUTHOR(s) V. Sarma Avva (Formerly A. V. Sharma)	8. CONTRACT OR GRANT NUMBER(s) F49620-80-C-0050
9. PERFORMING ORGANIZATION NAME AND ADDRESS Department of Mechanical Engineering N.C. A&T State University 1601 E. Market Street; Greensboro, NC 27411	10. PROGRAM ELEMENT, PROJECT, TASK AREA & WORK UNIT NUMBERS 61102F 2303/A3
11. CONTROLLING OFFICE NAME AND ADDRESS Department of the Air Force Air Force Office of Scientific Research (AFSC)/NC Bolling Air Force Base, D.C. 20332	12. REPORT DATE 30 September, 1982
	13. NUMBER OF PAGES 103
14. MONITORING AGENCY NAME & ADDRESS(if different from Controlling Office)	15. SECURITY CLASS. (of this report) Unclassified
	15a. DECLASSIFICATION/DOWNGRADING SCHEDULE

16. DISTRIBUTION STATEMENT (of this Report)

Approved for public release;
Distribution unlimited.

17. DISTRIBUTION STATEMENT (of the abstract entered in Block 20, if different from Report)

18. SUPPLEMENTARY NOTES

19. KEY WORDS (Continue on reverse side if necessary and identify by block number) composites, impact damage, residual strength, theoretical, experimental, rebound velocity technique, testing, graphite/epoxy laminate

20. ABSTRACT (Continue on reverse side if necessary and identify by block number)

Due to the advantage of high strength to weight ratio, composite materials are being increasingly used in the design of aircraft components and structures. One of the problems that needs to be studied in detail in such applications is the effect of projectile impact on the strength carrying ability of composite structures. The mechanism of impact-induced crack propagation is not fully understood, yet. In the past few years, numerous efforts have been made to predict theoretically the residual strength of the high performance fiber composite materials subjected to foreign object damage (FOD).

DD FORM 1 JAN 73 1473

Unclassified

SECURITY CLASSIFICATION OF THIS PAGE (When Data Entered)

Waddoups, et. al. [1]* have developed a method for predicting the strength of composite materials with an induced flaw. Whitney, et. al. [2], Nuismer, et. al. [3] have made use of point- and average-stress criteria to derive failure criteria for notched composite specimens. Various theoretical approaches to study the behavior of the notched composites based on linear elastic fracture mechanics and other methods have been reviewed by Yeow, et. al. [4]. Some of the investigations by Sharma [7, 8] were concerned in the development of graphite/epoxy composite failure thresholds leading to some design implications.

A theoretical model to predict the residual strength in laminated composite materials subjected to low velocity impact was developed by Husman, et. al. [5]. The model was developed based on an analogy between the damage caused by a projectile and an implanted flaw of known dimensions in composite laminate.

In the literature mentioned above, experimental validation of the analytical models was performed mostly with composite specimens subjected to tensile loads. Further, the upper and lower bounds of the damage threshold based on statistical methods, in general, have not been evaluated. Development of an analytical model followed by an experimental verification of the analytically predictable values in tension- and compression-loaded laminates was needed. With this need in the background, the following research work has been performed:

1. A method was established to measure the rebound velocity of the projectile using a stroboscope and a graphic polaroid camera.

2. A special fixture was designed to support the compression-loaded laminates against column-type buckling failures.

3. Established a residual strength curve as a function of impact energy in both the tension- and the compression-loaded laminates.

4. Evaluated the scatter in establishing the residual strength curve at three different projectile velocities.

5. Assessed the effect of pre-load on the residual strength at three different velocities.

6. Verified the validity of the theoretically predicted residual strength values experimentally both in the tension- and the compression-loaded laminates.

---

*Numbers in square brackets refer to references at the end.

FORWARD

This final technical report was prepared by V. Sarma Avva (formerly A.V. Sharma), Department of Mechanical Engineering, North Carolina Agricultural and Technical State University for the Directorate of the Chemical and Atmospheric Sciences, AFOSR (AFSC), Department of the Air Force, Bolling AFB, Washington, D.C. under a contract No. F49620-80-C-0050. The Program Manager was Dr. Donald R. Ulrich.

Principal Investigator:	V.S. Avva
Research Assistant:	H. L. Padmanabha
Technical Help:	Charlie Pinnix
Secretarial Help:	Dolores Ahrens

TABLE OF CONTENTS

SECTION		PAGE
I.	INTRODUCTION.	1
II.	REVIEW OF RELATED LITERATURE.	3
III.	ANALYTICAL MODEL.	10
IV.	SPECIMENS AND EXPERIMENTAL ARRANGEMENT. .	15
V.	EXPERIMENTAL PROCEDURE.	23
	1. Impact Tests in Tension	24
	a. Ultimate Strength Test.	24
	b. Impact Test on Pre-Loaded Specimens	25
	c. Impact Test Without Pre-Load. . .	25
	d. Impact Test With Pre-Load	26
	2. Impact Tests in Compression	26
	a. Ultimate Strength Test.	26
	b. Impact Test on Pre-Loaded Specimens	27
	c. Impact Test Without Pre-Load. . .	27
	d. Impact Test With Pre-Load	27
VI.	EXPERIMENTAL RESULTS AND ANALYSIS	29
	1. Tension Test.	29
	a. Ultimate Strength Test.	29
	b. Impact Test on Pre-Loaded Specimens	29
	c. Impact Test Without Pre-Load. . .	32
	d. Impact Test With Pre-Load (Scatter Study)	33

TABLE OF CONTENTS (continued)

SECTION		PAGE
	2. Compression Test.	35
	a. Ultimate Strength Test.	35
	b. Impact Test on Pre-Loaded Specimens	37
	c. Impact Test Without Pre-Load. . .	37
	d. Impact Test With Pre-Load (Scatter Study)	41
	3. Fracture Modes.	41
VII.	CONCLUSIONS	54
	REFERENCES.	56
	APPENDIX A.	57
	Tables	
	APPENDIX B.	86
	Linear Regression Analysis	
	APPENDIX C.	91
	Calculation of Rebound Velocity of Projectile	
	APPENDIX D.	93
	Calculation of Mean Stress Ratio and Standard Deviation of Mean	

LIST OF ILLUSTRATIONS

NO.		PAGE
1	SCHEMATIC DIAGRAM OF POST-IMPACT STRENGTH VS. PROJECTILE IMPACT.	11
2	SCHEMATIC REPRESENTATION OF SPECIMEN CONFIGURATION	16
3	SPECIMEN GRIPPING ARRANGEMENT	17
4	SCHEMATIC VIEW OF FIRING MECHANISM.	19
5	FIXTURE FOR COMPRESSION TEST.	21
6	PHOTOGRAPH OF A MATERIAL TESTING SYSTEM . .	22
7	NORMALIZED STRESS VS. K.E. OF PROJECTILE: TENSION	30
8	NORMALIZED RESIDUAL STRESS VS. K.E. OF PROJECTILE: TENSION.	34
9	SCATTER STUDY: TENSION.	36
10	NORMALIZED STRESS VS. K.E. OF PROJECTILE: COMPRESSION	38
11	NORMALIZED RESIDUAL STRESS VS. K.E. OF PROJECTILE: COMPRESSION.	40
12	SCATTER STUDY: COMPRESSION.	42
13	FRACTURE DUE TO ULTIMATE TENSILE STRESS . .	44
14	CATASTROPHIC FAILURE OF TENSION PRE-LOADED SPECIMEN	45
15	FRACTURE OF TENSION SPECIMEN WITH NO PRE-LOAD	46
16	PRE-LOADED TENSION SPECIMEN WITH COMPLETE PENETRATION	48
17	FRACTURE DUE TO ULTIMATE COMPRESSIVE STRESS.	49

LIST OF ILLUSTRATIONS (Continued)

NO.		PAGE
18	CATASTROPHIC FAILURE OF COMPRESSION PRE-LOADED SPECIMEN.	50
19	FRACTURE OF COMPRESSION SPECIMEN WITH NO PRE-LOAD.	52
20	PRE-LOADED COMPRESSION SPECIMEN WITH COMPLETE PENETRATION	53
21	PHOTOGRAPH SHOWING REBOUND PATH OF PROJECTILE AFTER IMPACT.	92

LIST OF TABLES

NO.		PAGE
I.	PANEL DATA (AVERAGE VALUES)	58
II.	ULTIMATE TENSILE STRESS-STRAIN DATA	59
III.	EXPERIMENTAL DATA: TENSION (PRE-LOADED SPECIMENS).	60
IV.	EXPERIMENTAL DATA: TENSION (NO PRE-LOAD)	66
V.	PRE-LOAD IMPACT TEST: TENSION (SCATTER STUDY)	70
VI.	ULTIMATE COMPRESSIVE STRESS-STRAIN DATA	74
VII.	EXPERIMENTAL DATA: COMPRESSION (PRE-LOADED SPECIMENS).	75
VIII.	EXPERIMENTAL DATA: COMPRESSION (NO PRE-LOAD)	80
IX.	PRE-LOAD IMPACT TEST: COMPRESSION (SCATTER STUDY)	83

SECTION I

INTRODUCTION

Due to the advantage of high strength to weight ratio, composites are being increasingly used in the manufacture of aircraft components and structures. One of the problems that required attention in their use is the strength degradation due to the impact of foreign objects. Jet engine fan blades, compressor blades and other aircraft structures are subject to hard-body impact like stones, rivets and other runway debris and soft-body impact like birds. Hard objects cause mainly local damage which may cause major degradation of strength or subsequent fatigue failure. Soft-body impact causes large deformations which might cause overall structural failure. The static residual strength of composites decreases as the velocity of impacting object increases. It reaches a minimum value at or near complete penetration. Beyond complete penetration, the residual strength is slightly higher than the minimum because the initial penetration causes more damage by removing material around the hole than the damage caused when the velocity is high enough to produce a clean hole.

There were numerous studies, both experimental and theoretical, associated with the behavior of the laminated composite materials subjected to low velocity projectile impact. Some of these pertinent studies are reviewed in the next

section. Some of the theoretical models proposed by various authors deal with the study of the effect of the implanted flaws of known dimensions on the strength carrying ability of the composite laminates. The extent of damage caused by the impact of a hard/soft object to the laminate resulting in its strength degradation is hard to determine precisely.

The purpose of the present study was to determine the failure threshold of graphite/epoxy composites with respect to the energy level of impact. In order to predict strength degradation due to the increase in the impact energy, an analytical model was developed. The strength values obtained by an analytical method were compared with the experimental values to verify the applicability of the model. Some typical tension and compression coupons were subjected to impact damage at various energy levels with a 12.7 mm (0.5") diameter aluminum projectile. The forward velocity range used in these tests was varied from 18.3 to 106.7 m/s (60 to 350 ft/s). To determine the actual kinetic energy absorbed by the specimen, the rebound velocity of the projectile was measured using a special technique as presented in this report.

SECTION II

REVIEW OF RELATED LITERATURE

A convenient method of predicting the static strength of composite materials with an induced flaw has been presented by Waddoups, et. al., [1].* Considering a notched composite specimen with a through the thickness crack of length 2a, the stress intensity factor for Griffith flaw in isotropic material was given by [1]

$$K_I = \sigma_r \sqrt{\pi(a + a_o)}$$

where σ_r = critical remote stress normal to the crack

$2a_o$ = characteristic or inherent flaw length in an unnotched specimen.

The stress intensity factor for an unnotched specimen was given by

$$K_I = \sigma_o \sqrt{\pi a_o}$$

where σ_o = ultimate strength of the unnotched specimen.

By combining the above two equations, the following relationship was obtained, viz.,

$$\frac{\sigma_o}{\sigma_r} = \sqrt{\frac{a + a_o}{a_o}} .$$

The value of a_o can be determined by performing a tensile

---

*Numbers in square brackets refer to references at the end.

test on an unnotched and a notched laminate. These tests provide the values for σ_o and σ_r. With the values of a_o and σ_o obtained from the tensile test, the value of σ_r can be determined for the same laminate with different sizes of implanted flaws.

Whitney and Nuismer [2, 3] have made use of the point stress criterion and the average stress criterion to derive alternate failure criteria for notched composite specimens. In the point stress criterion, it was assumed that failure occurs when the local stress at some distance a_1 away from the discontinuity is equal to or greater than the strength of the unnotched material, σ_o. Then,

$$\frac{\sigma_r}{\sigma_o} = \sqrt{1 - \zeta^2}$$

where $$\zeta = \frac{a}{a + a_1}$$

a = half crack length of induced flaw.

Whereas, in the average stress criterion, it was assumed that failure occurs when the average stress over a length d_o from the tip of the induced notch equals the unnotched laminate strength. From this theory, the following relationship was derived:

$$\frac{\sigma_r}{\sigma_o} = \sqrt{\frac{1 - \zeta_1}{1 + \zeta_1}}$$

where $\zeta_1 = \frac{a}{a + d_o}$.

Hence, $\frac{\sigma_r}{\sigma_o} = \sqrt{\frac{d_o}{2a + d_o}}$

The values of d_o and a_1 were determined by conducting tensile tests on an unnotched specimen and a notched specimen.

Several theoretical approaches for the analysis of the fracture behavior of notched-fiber composites were reviewed by Yeow, et. al. [4]. Some of the analytical results were compared with the experimental values obtained from uniaxial tests with graphite/epoxy tensile coupons containing center cracks.

In another study, Husman, et. al. [5] have developed an analogy between the damage caused by hard-particle impact and the damage due to an implanted flaw. This study, in part, states that for impact velocities less than the penetration velocity, the degree of damage depends on kinetic energy imparted to the specimen. In other words, the difference between the strain energy required to break an undamaged specimen and the strain energy required to break an impacted specimen is assumed to be proportional to the kinetic energy imparted and dissipated over some small volume of the specimen. The analytical model developed in this study was given by:

$$\sigma_r = \sigma_o \sqrt{\frac{W_s - K \bar{W}_{kE}}{W_s}}$$

where σ_r = Residual strength

σ_o = Static undamaged strength

W_s = Work/unit volume required to break an undamaged specimen

$\overline{W}_{kE}$ = Kinetic energy/unit thickness imparted to specimen

K = Effective damage constant.

The values of σ_o and W_s were determined by conducting a static tensile test on an unflawed specimen. The value of K was determined from the equation,

$$W_s - W_b = K \overline{W}_{kE}$$

where W_b = Work/unit volume required to break a damaged specimen.

W_b was determined by testing a specimen which was previously subjected to impact. Thus, experimental data obtained at one value of kinetic energy was used in determining the value of K. It was shown that the specimen width will affect the value of K whereas the specimen thickness will not significantly affect the K value. The analogy was shown to be valid by conducting some tension tests.

A study of impact damage of metal matrix composites was made by Awerbuch and Hahn [6]. To determine the post-impact residual strength analytically, it was proposed that

$$\frac{\sigma_r}{\sigma_o} = \frac{1}{Y(CV^2)} \sqrt{\frac{C_o}{CV^2 + C_o}}$$

where Y = Finite width correction factor for the damage size 2a.

V = Velocity of the projectile

C_o = Characteristic dimension of the damage zone

C = A material constant.

For impact velocities less than the ballistic limit velocity V_b, the value of C was determined by a semi-analytical method using an equation of the form, $a = CV^2$.

where a = Half damage size.

A least square fit of the damage size data obtained from actual tests was used in determining C. The incipient damage velocity V_o was neglected by the authors, for it was found to be too small compared to the velocity range studied.

For impact velocities greater than V_b, the value of C was determined by a purely analytical method using the equation, $C = \frac{d/2}{V_b^2}$

where d = diameter of the projectile.

Therefore, for $V > V_b$

$$\frac{\sigma_r}{\sigma_o} = \frac{1}{Y(d/2)} \sqrt{\frac{C_o}{(d/2) + C_o}}$$

The impact tests in this study were performed using a projectile with 4.5 mm (0.177 in.) diameter and a velocity range of 152.4 to 1219.2 m/s (500 to 4000 ft/s). It was shown that in boron/aluminum specimens the damage induced due to impact consisted of lateral and axial cracks causing a strength degradation of up to 50%, whereas the borsic/titanium specimens exhibited localized plastic deformation and strength degradation of 20%. A comparison between analytical predictions and experimentally observed values of post-impact residual strengths was made.

An experimental study on the strength degradation of composite sandwich specimens subjected to low velocity projectile impact was conducted by Sharma [7]. Failure threshold curves for sandwich-type graphite/epoxy composite specimens with laminate configurations of $(\pm 45, 0_4)_s$, $(\pm 45, 90, 0)_s$ and $(90, \pm 45, 0)_s$ were generated. Impact tests were conducted on specimens subjected to tensile and compressive loads in the velocity range of 17 to 64 m/s (56 to 210 ft/s). It was shown that the strength degradation due to impact is dependent on the laminate configuration and the fiber/matrix combination.

In another investigation by Sharma [8], the effect of length to width aspect ratio and the laminate thickness on the buckling strain of graphite/epoxy composites was studied. Low velocity impact tests were performed on compression specimens using 16 ply- and 32 ply-thick

laminates and a $(\pm 45, 0, 90)_s$ basic stacking sequence. It was shown that, at constant thickness, the length to width aspect ratio has no significant effect on the buckling strain values at failure caused by the projectile impact. It was also reported that as the velocity of impacting projectile increases, the influence of the thickness on the buckling strain decreases.

With the results of the preceding review in the background, an attempt was made to develop an improved analytical model to predict the strength degradation of the graphite/epoxy composites subjected to low velocity projectile impact. An aluminum sphere of 1.27 cm (0.5 in.) diameter was used as a projectile to simulate the effect of the impact of runway debris, hail, etc. Aluminum is considered to have the same density as the density of the runway debris such as a rock. Linear regression analysis was adopted to determine certain material constants to be defined later. A method was established to determine the rebound velocity of the projectile after impacting the specimen. Finally, the experimental results were compared with the theoretical values.

SECTION III

ANALYTICAL MODEL

In resin matrix composites, small object impact causes local damage in the impacted area which appears in the form of indentation, perforation, delamination and spallation. Damage thus induced causes reduction of strength of the material. Post-impact strength degradation with respect to impact velocity [6] is schematically represented in Figure 1. At low impact velocities, the damage caused is insignificant to result in any reduction of the residual strength. Beyond a certain value, a steep reduction of strength takes place. Velocity at this point is referred to as the threshold damage velocity. With increase in velocity, the residual strength decreases until it reaches a minimum, where the impact causes maximum damage. This is the ballistic limit velocity. Further increase in impact velocity results in complete penetration of the projectile. The residual strength will be slightly higher than the minimum and is equal to the strength of the specimen with a drilled hole of the same size. Beyond the ballistic limit, residual strength is independent of impact velocity.

Due to the fact that damage does not occur at velocities less than the threshold damage velocity, it may be assumed

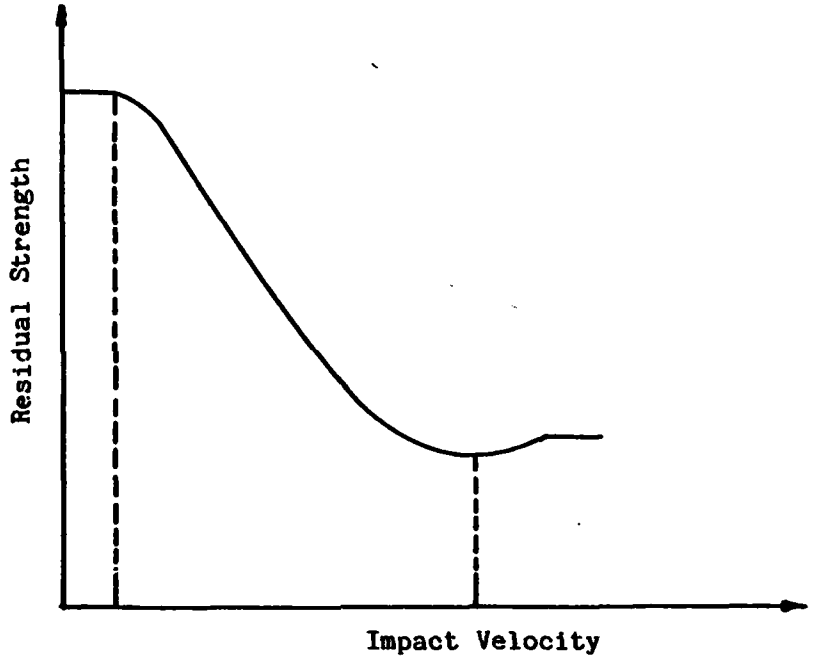

Figure 1. Schematic Diagram of Post-Impact Residual Strength vs. Projectile Impact

that the damage is proportional to the difference between the kinetic energy of impact and the threshold damage kinetic energy. Therefore, the preceding statement may be expressed as [9]

$$c = k\,(W - W_o) \tag{1}$$

where c = damage as an effective through the thickness crack of length 2c.

k = constant depending on the material and the laminate

W = kinetic energy of impact per unit thickness

W_o = threshold damage kinetic energy per unit thickness.

The average stress criterion developed by Whitney and Nuismer [2] for an isotropic or orthotropic laminate is given by

$$\frac{\sigma_N^{\infty}}{\sigma_o} = \sqrt{\frac{1 - \zeta_1}{1 + \zeta_1}} \tag{2}$$

where σ_N^{∞} = Failure stress of an infinite plate containing a crack of length 2c.

σ_o = Failure stress of an unnotched plate

$\zeta_1 = \dfrac{c}{c + a_o}$

a_o = Characteristic dimension adjacent to discontinuity.

Substituting for ζ_1 in equation (2),

$$\frac{\sigma_N^{\infty}}{\sigma_o} = \sqrt{\frac{a_o}{2c + a_o}} \tag{3}$$

The equations (1) and (3) can be combined resulting in the following:

$$\frac{\sigma_N^{\infty}}{\sigma_o} = \sqrt{\frac{a_o}{2k(W-W_o) + a_o}},$$

or

$$\frac{\sigma_N^{\infty}}{\sigma_o} = \sqrt{\frac{1}{\frac{2k}{a_o}(W-W_o) + 1}} \qquad (4)$$

Assuming $\sigma_N^{\infty} = \sigma_r$, residual strength of the specimen

and $\frac{k}{a_o} = K$, a constant

the equation (4) can be re-written in the following form:

$$\frac{\sigma_r}{\sigma_o} = [2K(W-W_o) + 1]^{-\frac{1}{2}} \qquad (5)$$

The above relationship can be used to predict the residual strength of a laminate for different values of kinetic energy. In order to determine the values of 2K and W_o, the equation (5) is re-written in linear form as:

$$y = ax + b$$

where $y = (\sigma_o/\sigma_r)^2$

$x = W$

$a = 2K$

$b = 1 - 2KW_o$

The ultimate strength σ_o and the post-impact residual strength σ_r at different velocities are to be determined

by performing tests on a few specimens. Using linear regression analysis (Appendix B), a best fit is obtained for the data and the values for 2K and W_o are thus determined. These values are used in equation (5) to predict the residual strength at any velocity of impact.

SECTION IV

SPECIMENS AND EXPERIMENTAL ARRANGEMENT

The graphite/epoxy composite material used for both the tension and the compression test specimens is Thornell 300/Rigidite 5208. These specimens have 16 plies with a laminate stacking sequence of $(45_2, -45_2, 0_2, 90_2)_s$. The nominal cured thickness of each lamina is 140×10^{-6}m (0.0055 in.) and the nominal width of each specimen is 7.5 cm (3 in.). Other nominal dimensions of the specimen and gripping arrangement are shown in Figures 2 and 3. Panel data is indicated in Table 1.

All the specimens were fabricated according to specifications by private companies. A brief outline of the procedure used by fabricators is given here.

The specimens were cut from large panels which had been autoclave cured as per the pre-peg manufacturer's suggested curing procedure. Representative sections of all panels were inspected using c-scan for voids. These sections were tabbed and the tabbed sections were pre-cut by a diamond saw to approximately 3.2 mm (1/8 in.) over-size. Individual specimens were then edge ground to a nominal width of 7.5 cm (3 in.) with end to end variation of 0.05 mm (0.002 in.) or less.

The tab length of compression specimens supplied

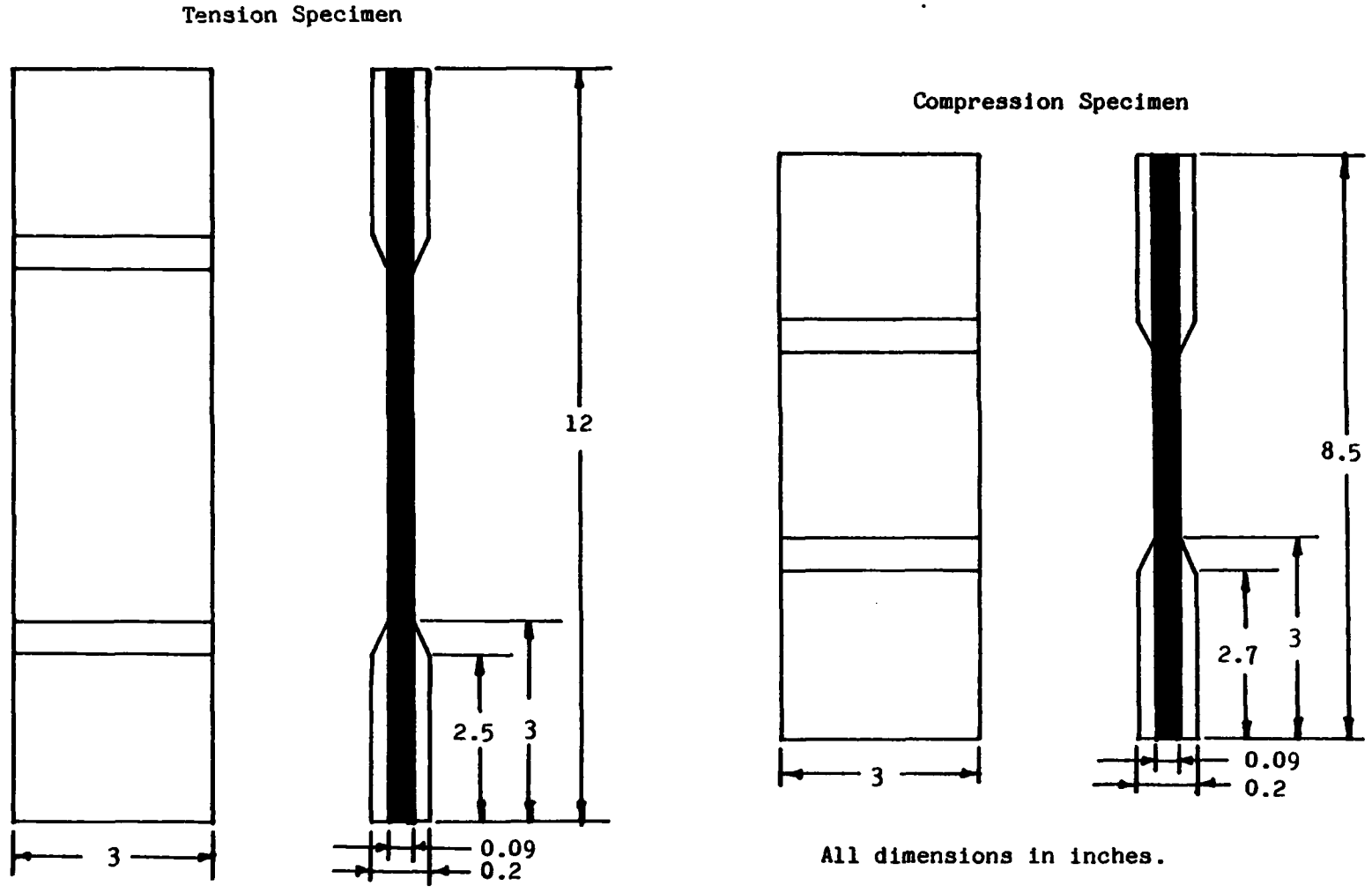

Figure 2. Schematic Representation of Specimen Configuration.

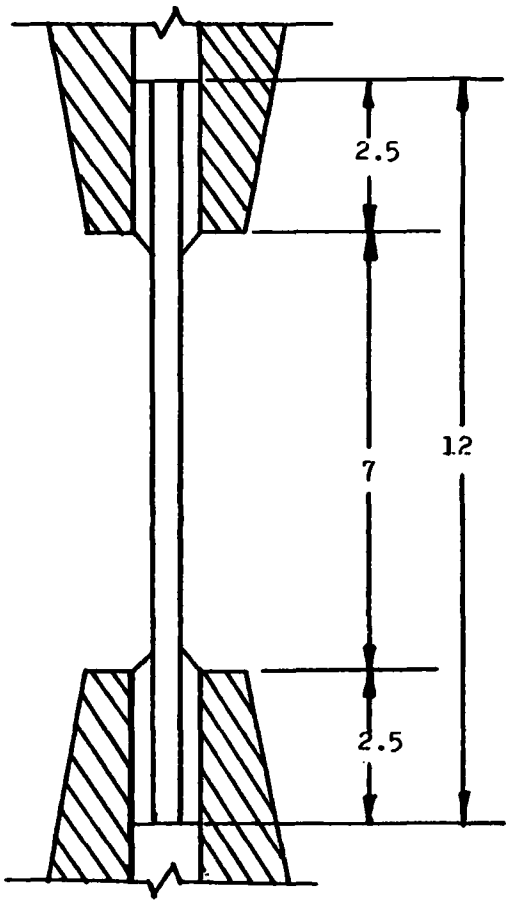

Tension Specimen

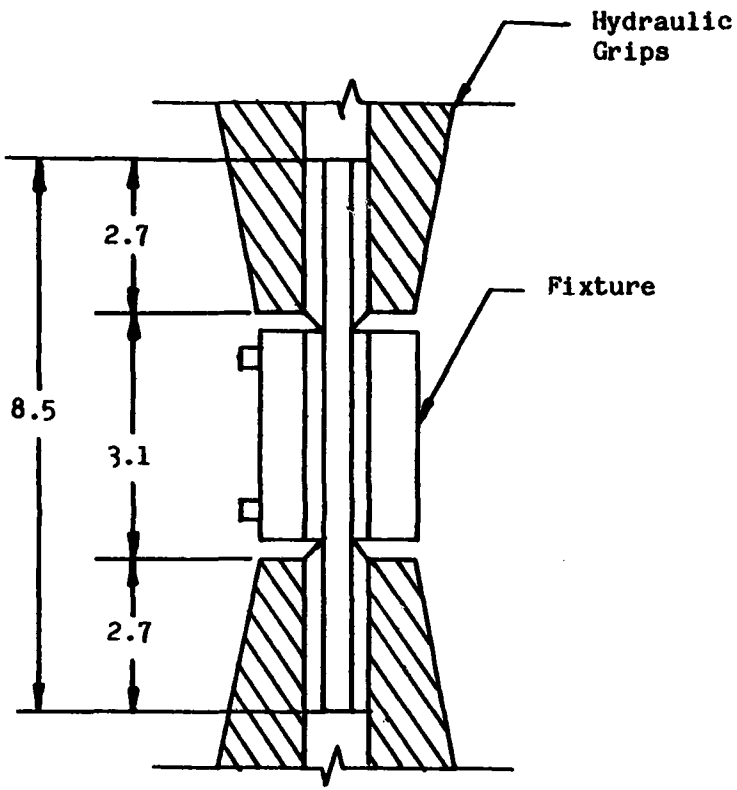

Compression Specimen

Figure 3. Specimen Gripping Arrangement.

exceeded the support length of the hydraulic grips. In order to meet the gripping and the side support fixture dimensions, the tab length of compression specimens was reduced and made equal to the tab length of tension specimens (Figure 2).

A schematic view of the projectile firing mechanism is shown in Figure 4. An air supply line is connected to a reservoir through a butterfly valve. A (gun) barrel connected to the reservoir acts as a smooth guide to the projectile. Two photo-diodes located at 15.24 cm. (6 in.) apart at the other end of the barrel are connected to an electronic counter. As the projectile travels through the barrel, light beams emitted by the photo-diodes are interrupted. Electronic counter starts when the first light beam is interrupted by the projectile and stops when the second light beam is interrupted. Thus, the counter records the time taken by the projectile to travel a distance of 15.24 cm (6 in.) and hence the average forward velocity of the projectile can be determined. A solenoid valve is used to release the compressed air from the reservoir which in turn propels the projectile through the barrel.

The rebound velocity of the projectile after impact was determined by using a stroboscope and a graphic polaroid camera. The frequency range of the stroboscope

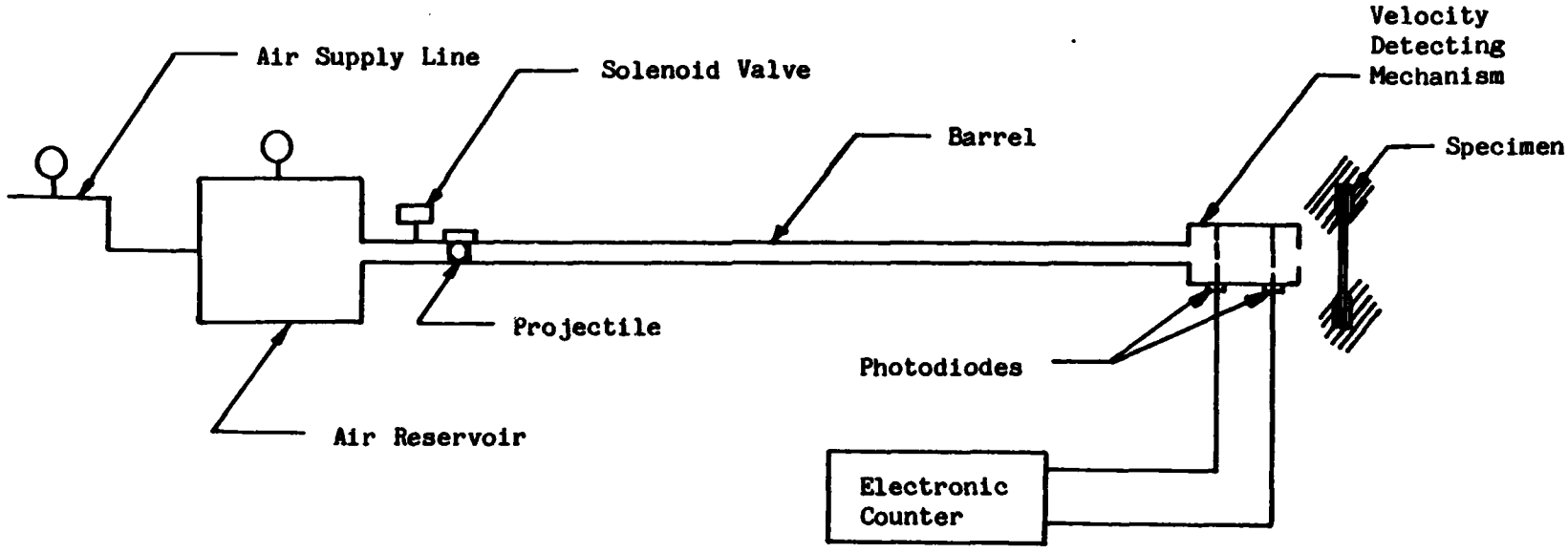

Figure 4. Schematic View of Firing Mechanism.

used was 110 to 150,000 flashes/min. A Polaroid, Polapan Land Film, Type 52, 400 ASA was used to photograph the rebounding path of the projectile. A dark screen embedded with a calibrated rectangular grid was placed by the side of the specimen. The screen was positioned close to the specimen so that it provided a background to projectile photographed during the impact. Rebound velocity was calculated by knowing the frequency of the flashing and the average distance between consecutive projectile positions that were frozen on the Polaroid film. There may be some error involved in the calculation of the rebound velocity since the trajectory of the projectile was photographed in one plane only. However, considering the magnitude of the rebound velocity {6-12 m/s (20-40 ft/s)} that was recorded as compared to the forward velocity, the error was considered to be negligible.

In compression tests, a special fixture (Figure 5) was used to prevent the specimen from column-type premature failure. The roller bars made line contact along the length on both faces of the specimen and provided firm but nonpenetrating support. This arrangement prevented buckling and stress concentration in the specimen.

The testing of specimens was performed on a standard closed-loop hydraulic material test system, Figure 6. The capacity of the equipment used was 250 kN (55 kips).

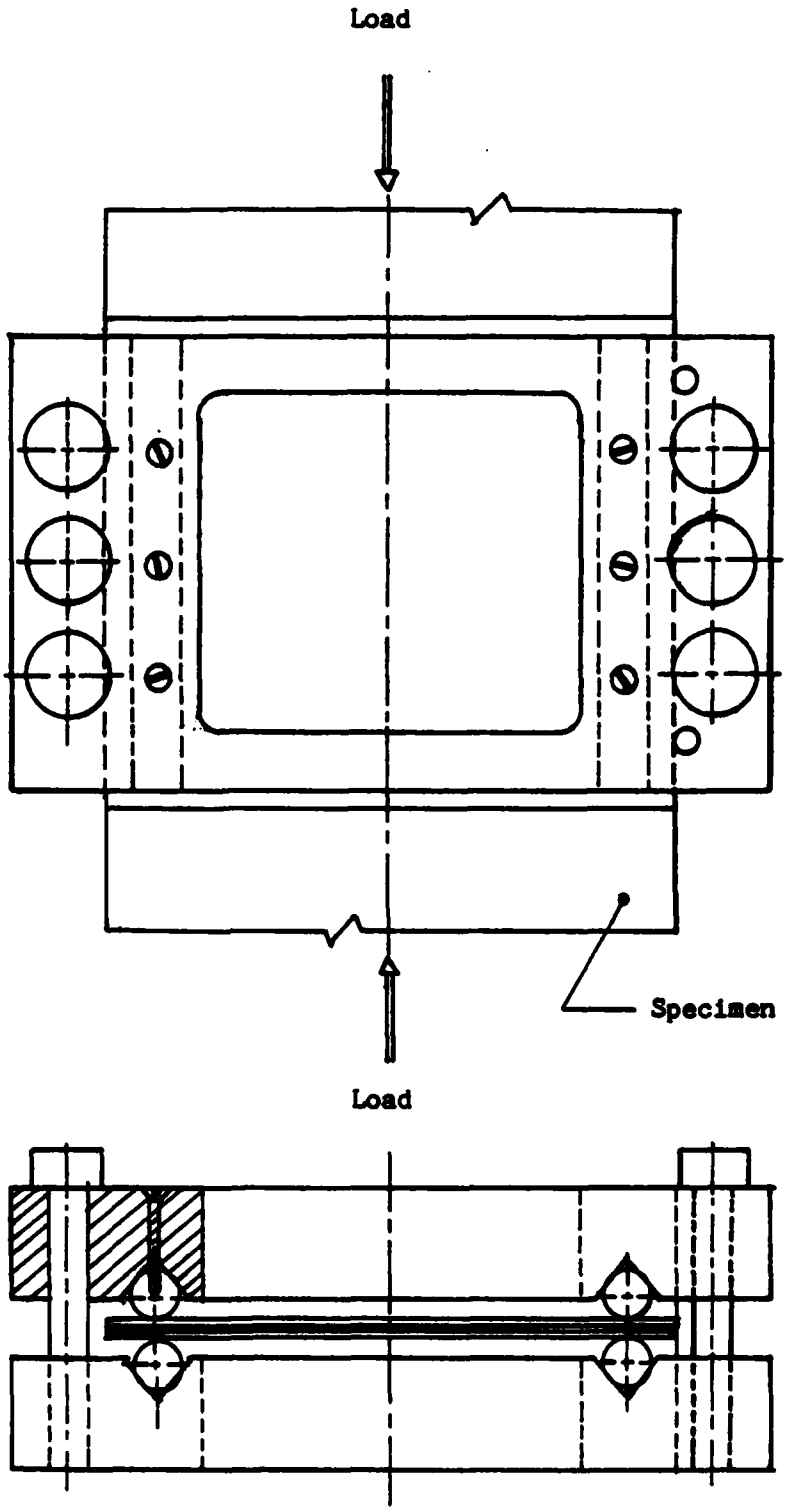

Figure 5. Fixture for Compression Test

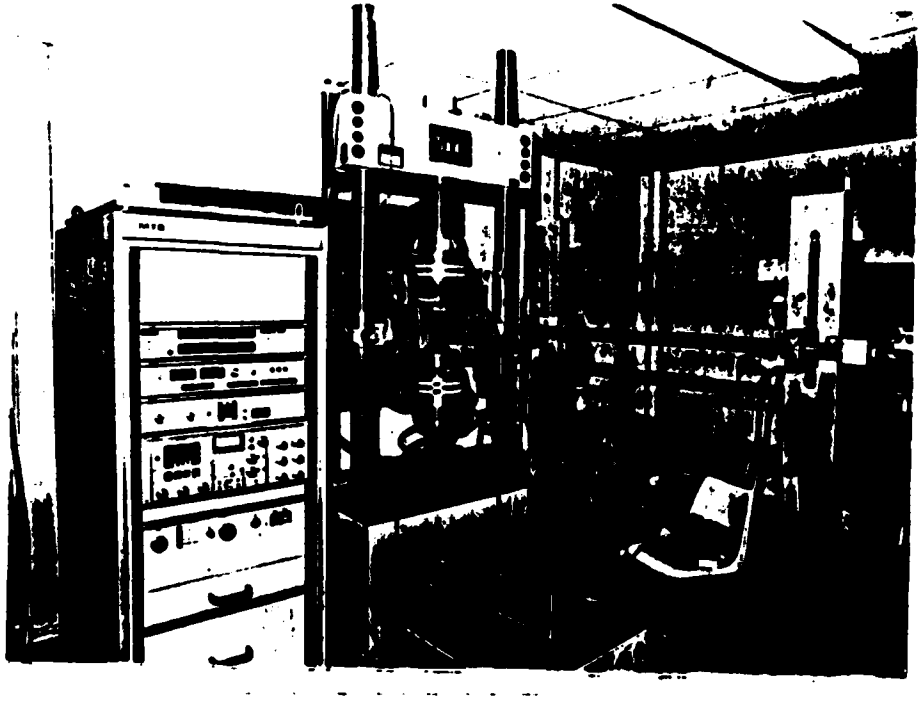

Figure 6. Photograph of a Material Testing System

SECTION V

EXPERIMENTAL PROCEDURE

The dimensions of all the tension and the compression test specimens were measured before conducting the tests. The tension specimens were numbered by the fabricator indicating the panel number and the position of the specimen within the panel. The location of the compression specimen was also identified. The tension and the compression specimens were fabricated by two different vendors. In order to ensure equal probability of selecting the specimens from all the panels, the techniques underlying the principles of randomization were used. In both the tension and the compression, tests were performed in four different stages; viz., (a) ultimate strength test to record stress-strain data, (b) impact tests on pre-loaded specimens to generate a failure threshold curve, (c) impact tests without pre-load at three different velocities to record post-impact residual strength, (d) impact tests with pre-load at three different velocities to study residual strength scatter and to compare the data with that of part (b).

In order to compare the theoretical and the experimental results, a method was established to determine the rebound velocity of the projectile. The set-up used for this purpose was explained in the

previous section. With the lights turned off in the test area, a flashing beam of light of pre-determined frequency from the stroboscope was directed into the space normal to the plane of the specimen and the camera was focussed into the same space. The camera shutter was opened simultaneously with the release of the projectile by operating the solenoid valve switch and closed after the rebound of the projectile takes place from the specimen. To ensure uniform duration of opening of the shutter for all specimens, the shutter was held open until numbers from 3 to 1 were counted and then closed. The number of images of the projectile in the rebound path and the distance between the images was noted from the photograph. A typical calculation of the rebound velocity is shown in Appendix C.

Impact Tests In Tension

Ultimate Strength Test:

Six specimens were tested for determining the ultimate strength. Two strain gages, one on each face of the specimen, back-to-back, were bonded at the center. The strain gage bridge completion network was arranged to record the average axial strain only, and the bending strains, if any, were eliminated in the recording. The specimens were held between the hydraulic grips for the

full length of the tabs and the tensile load was applied to achieve a strain rate of 2% per minute until the specimen failed. The load and the corresponding axial strain data were recorded. Table II shows the ultimate stress-strain data.

Impact Test on Pre-Loaded Specimens:

These tests were conducted to determine the failure threshold level of the composite laminate. The specimens were subjected to different pre-loads in tension and then were impacted by the projectile at velocities ranging from 18.6 to 106.7 m/s (61 to 350 ft/s). Some of the specimens failed catastrophically upon impact. Those specimens that survived the impact were subjected to continued loading until failure occured and the residual strength was found. The complete penetration of the laminate occured at a projectile velocity of 88.4 m/s (290 ft/s) or higher depending on the magnitude of the pre-load. The experimental data is presented in Table III.

Impact Test Without Pre-Load:

In these tests, the specimens were first impacted with one of the three projetile velocities at 30.5 m/s (100 ft/s), 61 m/s (200 ft/s), or 91.5 m/s (300 ft/s) and then loaded in tension until failure. The data obtained from these tests is presented in Table IV. It

may be noted that the exact value of the predetermined forward velocity could not be achieved everytime due to the design characteristics of the projectile release mechanism. Therefore, the data presented in the above Table is for such velocities which are close to the predetermined velocities.

Impact Test With Pre-Load:

These tests were performed at the same three impact velocities as in the previous case. The specimens were subjected to the projectile impact after pre-loading them in tension to a load level slightly below and above the failure threshold values. The data presented in Table V shows the residual strength scatter of the specimens at these velocities.

Impact Tests in Compression

Ultimate Strength Test:

The average ultimate strength of the laminate was found from testing five specimens in compression. A procedure similar to the tension tests was used to evaluate the strains in compression tests. The compression fixture shown in Figure 5 was used to prevent specimens from column-type buckling failure. The roller bars in the fixture provide a line contact along the length on both the faces of the specimen. The fixture was attached to the specimen with just enough pressure

to keep it in position from sliding. The fixture-induced stress concentration effects were thus minimized. The specimen was held between two hydraulic grips and the compressive load applied at a strain rate of 2% per minute until failure occured. The ultimate stress-strain data is shown in Table VI.

Impact Test on Pre-Loaded Specimens:

The test procedure in compression was similar to that in tension. The specimens were pre-loaded in compression and then impacted at different velocities. Those specimens that did not fail upon impact were tested to determine the residual strength. Complete penetration of the laminate was observed at velocities of 80 m/s (262 ft/s) and beyond. The Table VII shows the experimental data for this series of tests.

Impact Test Without Pre-Load:

These tests were conducted at the same three velocities as in tension tests. The results obtained at velocities close to the three predetermined velocities are presented in Table VIII.

Impact Test With Pre-Load:

These tests were performed to study the residual strength scatter under compressive loads at the three velocities of 30.5 m/s (100 ft/s), 61 m/s (200 ft/s) and 91.5 m/s (300 ft/s). As in tension tests, the

specimens were pre-loaded in compression to various loads slightly below and above the failure threshold values before impacting. The Table IX shows the data obtained from these tests.

In all the tension and the compression tests, the load was applied at a uniform strain rate of 2% per minute. The rebound velocity of the projectile was determined in all the impact tests except when complete penetration occurred.

SECTION VI

EXPERIMENTAL RESULTS AND ANALYSIS

Tension Test

Ultimate Strength Test:

To determine the average tensile ultimate stress and the strain of the laminate, static tests were conducted on six specimens. Table II presents the experimental data recorded. The highest ultimate strength, σ_o, observed was 421.2 GPa (61.1 ksi) and the lowest was 383.4 GPa (55.6 ksi). The corresponding ultimate strains were 1% and 0.8%, respectively. The average ultimate stress and strain values are 398.2 GPa (57.8 ksi) and 0.9%, respectively. This average ultimate strength value was used in the subsequent numerical calculations.

Impact Test on Pre-Loaded Specimens:

Impact tests on specimens subjected to the tensile pre-loads were conducted. The experimental results are shown in Table III. Some of the specimens failed near the tabs and showed very low values of the residual strength after impact. This was attributed possibly to inaccurate specimen mounting techniques. Such values are not shown in the table. The normalized stress as a function of the kinetic energy of the projectile per unit thickness of the specimen is shown in Figure 7.

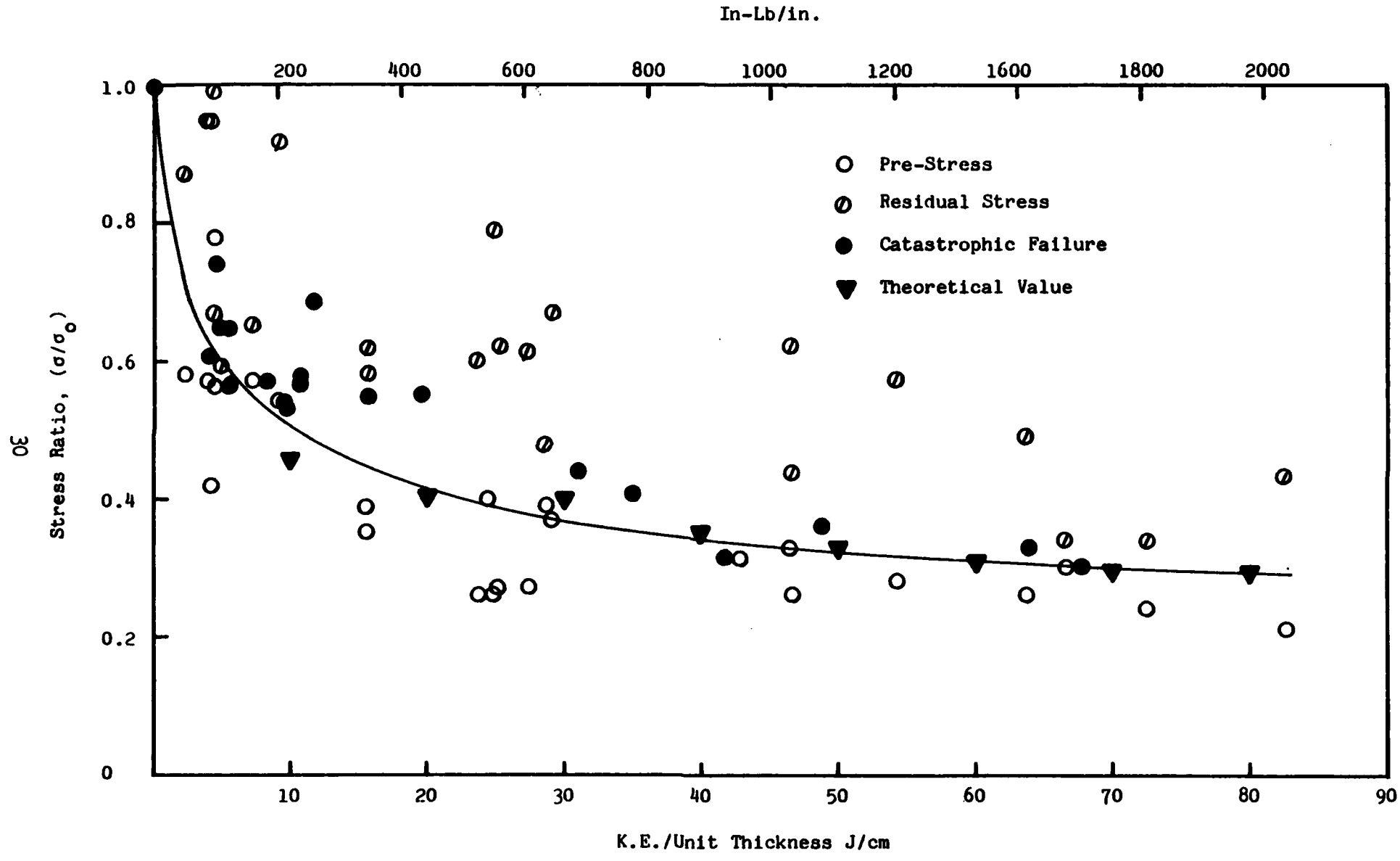

Figure 7. Normalized Stress vs. K.E. of Projectile: Tension.

The normalized pre-stress is indicated by an open circle, the normalized residual stress is shown by a circle with a slash in the center and the stress at catastrophic failure upon impact is represented by a darkened circle. A faired curve through the data points indicating a failure threshold for the laminate is drawn. The points shown above the faired curve represent either a catastrophic failure or a failure due to the continuation of loading (residual stress) after impact and the points below the faired curve represent pre-stress at impact but no failure. It may be noted that there are some stray data points in both the regions. This could be due to either mis-alignment of the specimen while loading or to the existence of some inherent damage in some of the virgin specimens. Since the number of these points is small compared to the total number of specimens tested, they may be neglected.

The faired curve in Figure 7 may be divided into three parts. In the first part, up to an impact energy level of 3 J/cm (67.4 in-lb/in), the stress ratio reduced very rapidly from 100% to about 70%. In the second part, between 3 J/cm (67.4 in-lb/in) and 70 J/cm (1574 in-lb/in), the reduction in the stress ratio is gradual from 70% to about 30%. In the third part of the curve, beyond 70 J/cm (1574 in-lb/in), there is no further reduction in the

stress ratio with an increase in the impact energy. This observation of the behavior of the failure threshold for the laminate under consideration may be interpreted to mean that the strength carrying ability of the laminated composite is dependent on the magnitudes of the pre-load and the impact energy applied to the specimen up to a point closer to the projectile penetration velocity. Beyond this point, the laminate failure is independent of the projectile impact energy.

In order to determine the stress-ratio at different impact energy levels analytically using the model as suggested in Section III, the values of 2K and W_o were determined using linear regression analysis as shown in Appendix B. For the particular test under consideration, it was found that 2K = 0.111 and W_o = -23.47 J/cm. The theoretical values of the stress ratio are also plotted as shown in Figure 7 and show good agreement with the faired curve drawn from experimental values.

Impact Test Without Pre-Load:

As mentioned earlier, the impact tests without pre-load were conducted at velocities close to 30.5 m/s (100 ft/s), 61 m/s (200 ft/s), and 91.4 m/s (300 ft/s). The results obtained are shown in Table IV. The mean σ_r/σ_o and the standard deviation of the mean σ_r/σ_o at these three impact energy levels were determined. A

sample calculation is shown in Appendix D. From these calculations, the following results were obtained:

Mean Kinetic Energy/Thickness J/cm in-lb/in	Mean Residual Stress, σ_r GPa ksi	Mean Stress ratio, σ_r/σ_o	Standard Deviation of mean σ_r/σ_o
5.7 129.3	356.4 51.7	0.90	±0.02
22.8 512.6	257.5 37.4	0.65	±0.02
54.7 1229.7	219.3 31.8	0.55	±0.04

From the above values, the normalized residual strength as a function of K.E./unit thickness is plotted as shown in Figure 8. A comparison of Figures 7 and 8 indicates that the total strength reduction due to impact without pre-load is 43% and with pre-load, it is 70%. From this observation, one may infer that the combination of pre-load and impact causes greater damage to the material than impact alone without any pre-load.

In the present case, the values of $2K = 0.035$ and $W_o = -9.71$ J/cm were calculated by using the linear regression technique. The theoretical values of (σ_r/σ_o), plotted in Figure 8, show good agreement with the experimental values.

Impact Test With Pre-Load (Scatter Study):

These tests were performed to study the scatter in the residual stresses and the catastrophic failure stresses at

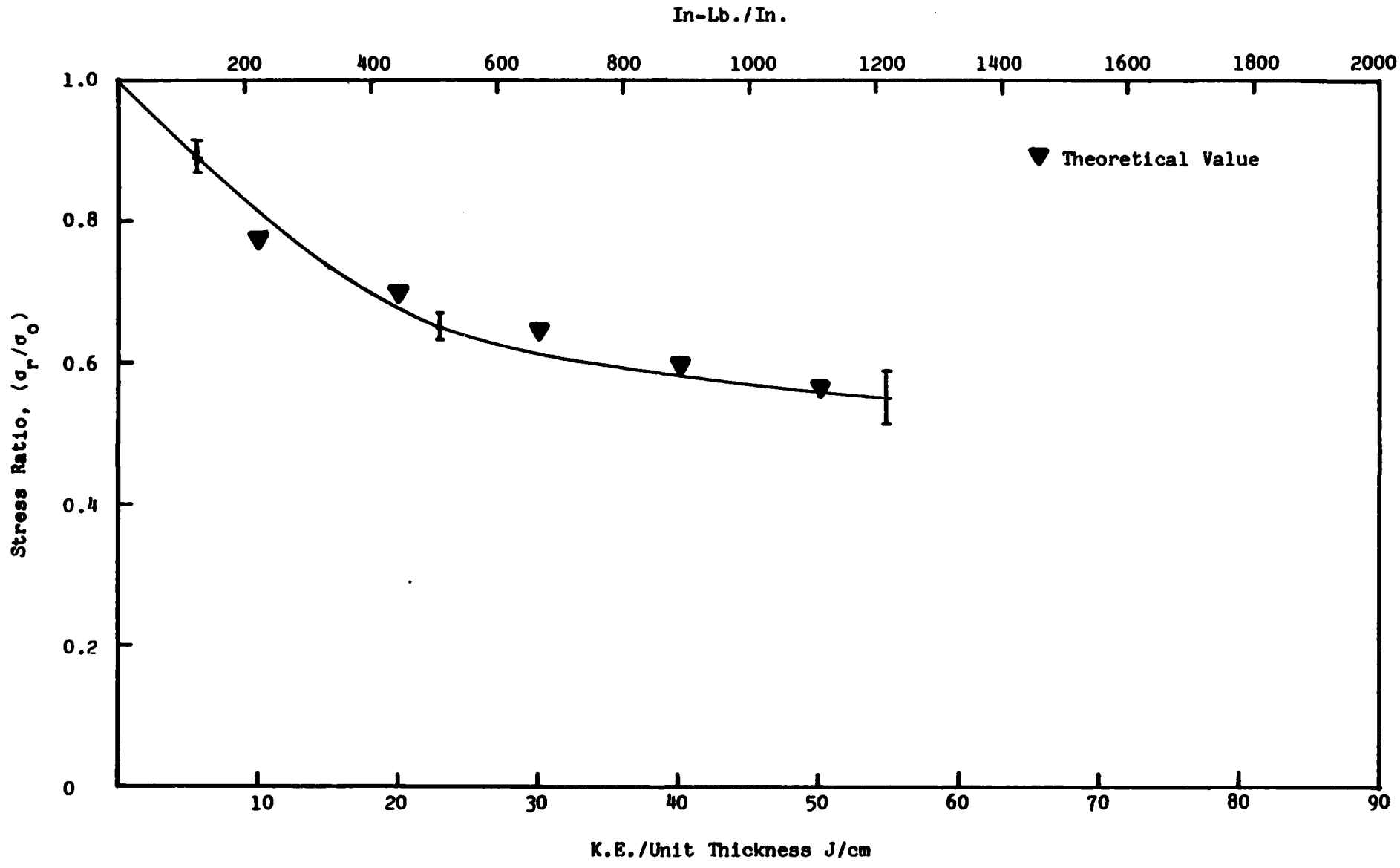

Figure 8. Normalized Residual Stress vs. K.E. of Projectile: Tension

the three impact energy levels. The results obtained are presented in Table V. These values are also plotted as shown in Figure 9. For the purpose of comparison, the faired curve drawn in Figure 7 is shown again in Figure 9. Most of the specimens impacted at a pre-stress above the faired curve had catastrophic failure, and those impacted below the faired curve survived. Therefore, one can infer that the faired curve is a true representation of the failure threshold for these laminates. It can be observed from Figure 9 that the scatter of residual stress points was high at an energy level of 6.2 J/cm (148.5 in-lb/in) whereas at 24.9 J/cm (556.5 in-lb/in) and 56.6 J/cm (1263.8 in-lb/in) these points were found to be in the vicinity of the faired curve.

Compression Test

Ultimate Strength Test:

Table VI shows the results of ultimate strength tests in compression. Out of the five specimens tested, the highest compressive strength, σ_o recorded was 328.2 GPa (47.6 ksi), and the lowest was 293.0 GPa (42.5 ksi). The average ultimate stress was 308.5 GPa (44.7 ksi). All the specimens tested have shown an equal ultimate strain of 0.6%. The ultimate stress and strain values in compression were found to be lower compared to the tensile stress and the strain values of 398.2 GPa (57.8 ksi) and 0.9%, respectively.

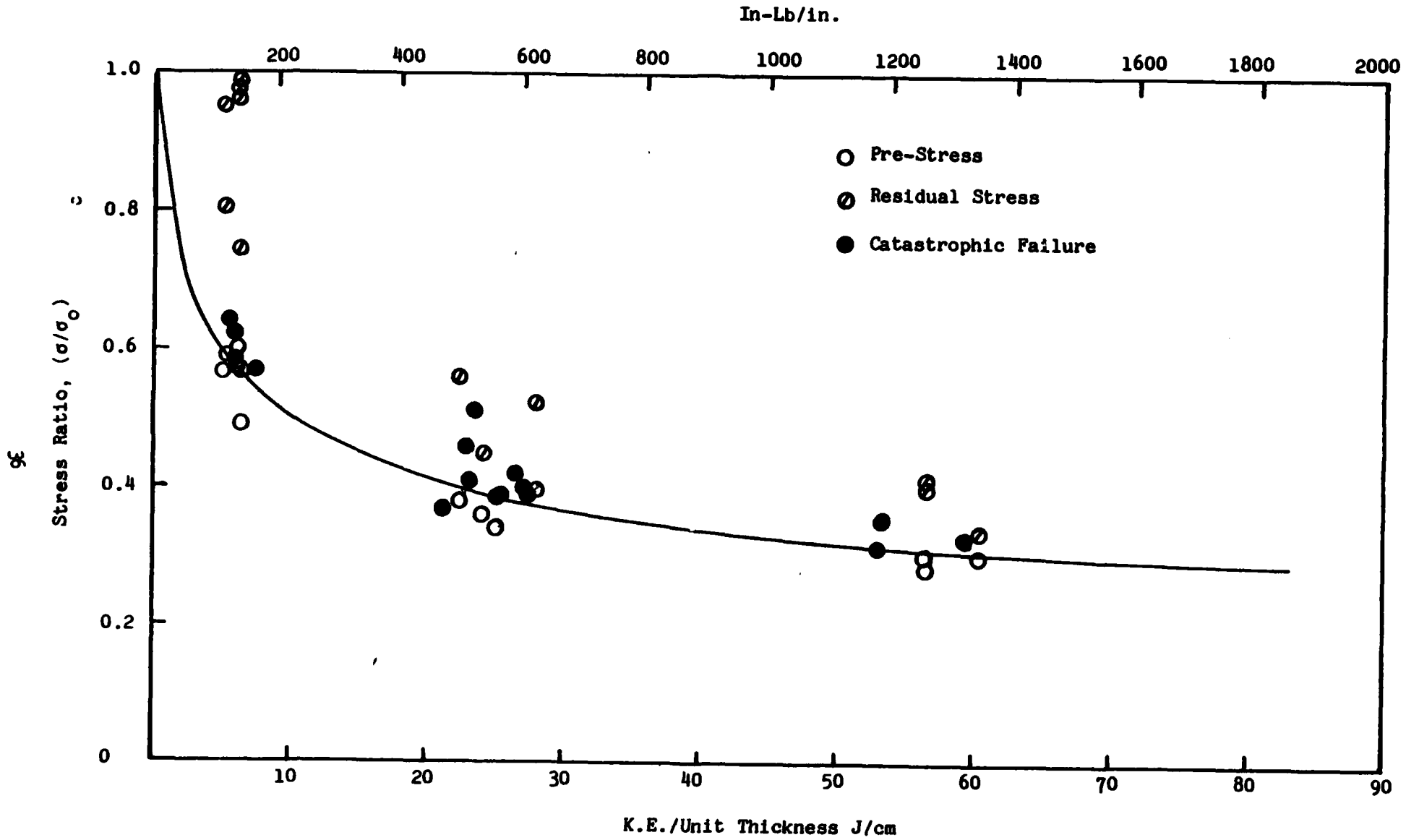

Figure 9. Scatter Study: Tension

Impact Test on Pre-Loaded Specimens:

The experimental data obtained from these tests is presented in Table VII and these values are plotted as shown in Figure 10. Symbols used for plotting are the same as explained in the tension tests. A faired curve which demarcates the survival zone from the failure zone is shown in Figure 10. In the first part of the curve between 0 and 13 J/cm, there is a rapid strength degradation of about 60% of the ultimate strength. In the second part, the reduction in the strength with increase in the impact energy is very gradual. The residual strength in compression reduced to 32% of the ultimate strength compared to 30% observed in the tension specimens.

Using the linear regression, the values of $2K = 0.073$ and $W_o = -53.85$ J/cm were obtained. The stress ratios at different impact energy levels were calculated using these values of 2K and W_o in the analytical model as discussed in Section III. The theoretical values thus obtained are also plotted as shown in Figure 10 and show good agreement with the faired curve drawn based on the experimental values.

Impact Test Without Pre-Load:

These tests were conducted at the same three velocities, i.e., velocities close to 30.5 m/s (100 ft/s), 61 m/s (200 ft/s) and 91.4 m/s (300 ft/s) as in tension

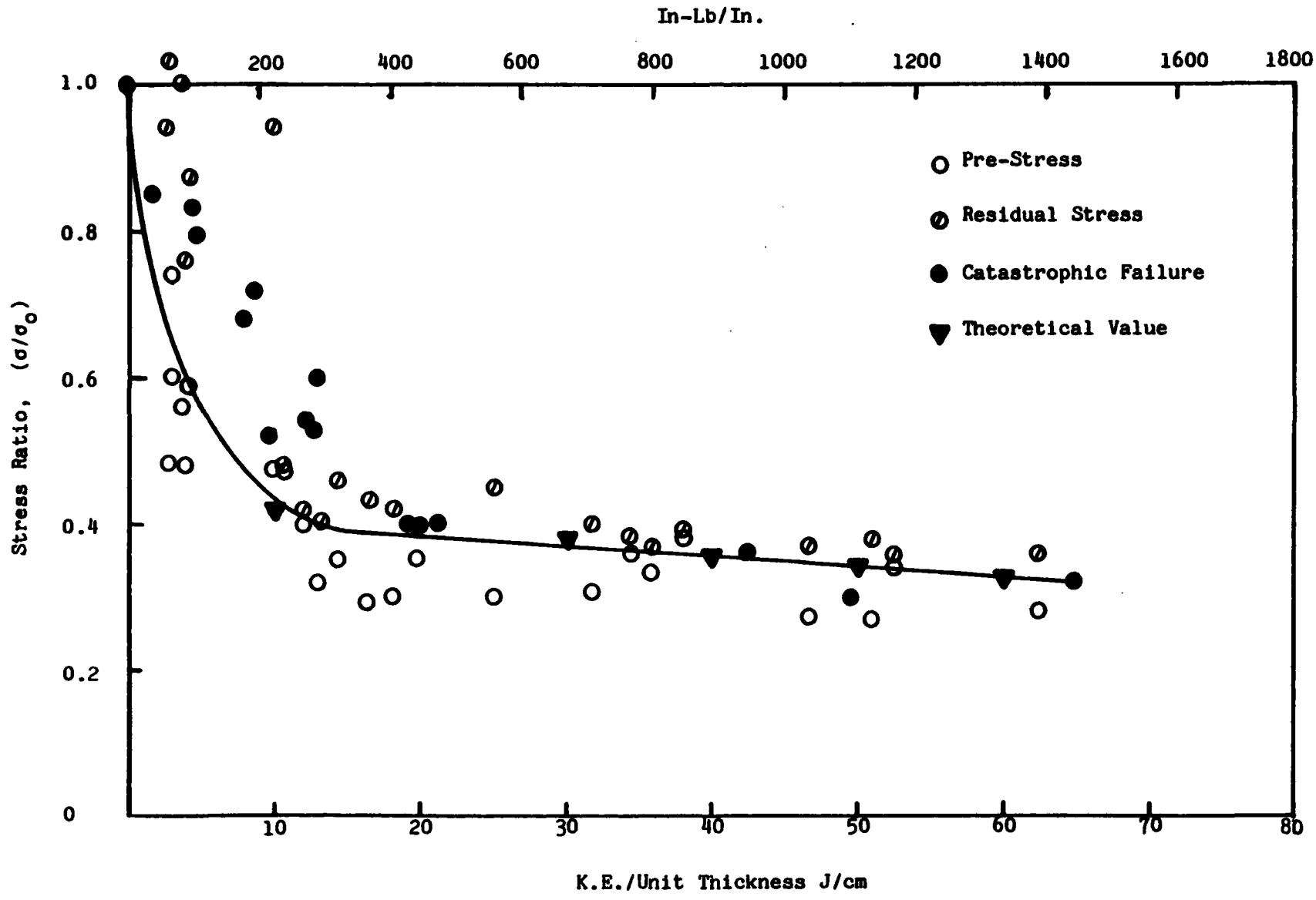

Figure 10. Normalized Stress vs. K.E. of Projectile: Compression

tests. The results obtained are tabulated as shown in Table VIII. From these values, the mean σ_r/σ_o and the standard deviation of the mean σ_r/σ_o were calculated and are given below:

Mean Kinetic Energy/Thickness J/cm in-lb/in	Mean Residual Stress, σ_r GPa ksi	Mean Stress Ratio, σ_r/σ_o	Standard Deviation of mean σ_r/σ_o
5.3 119.1	257.8 37.4	0.84	±0.01
23.7 532.8	133.7 19.4	0.43	±0.01
58.7 1319.6	111.0 16.1	0.36	±0.01

With the above values, the normal residual strength as a function of K.E./unit thickness was plotted as shown in Figure 11. A comparison of Figures 10 and 11 shows that the residual strength of specimens impacted without pre-load is much higher than pre-loaded specimens up to an impact energy of 25 J/cm. Beyond this impact energy level, the difference is only about 3%. Whereas in tension test, this difference is fairly uniform at all impact energy levels.

From the linear regression analysis, the values of $2K = 0.12$ and $W_o = -5.192$ J/cm were obtained. The stress ratios at different values of W were calculated using the analytical model. The theoretical values plotted in Figure 11 show good agreement with the experimental values.

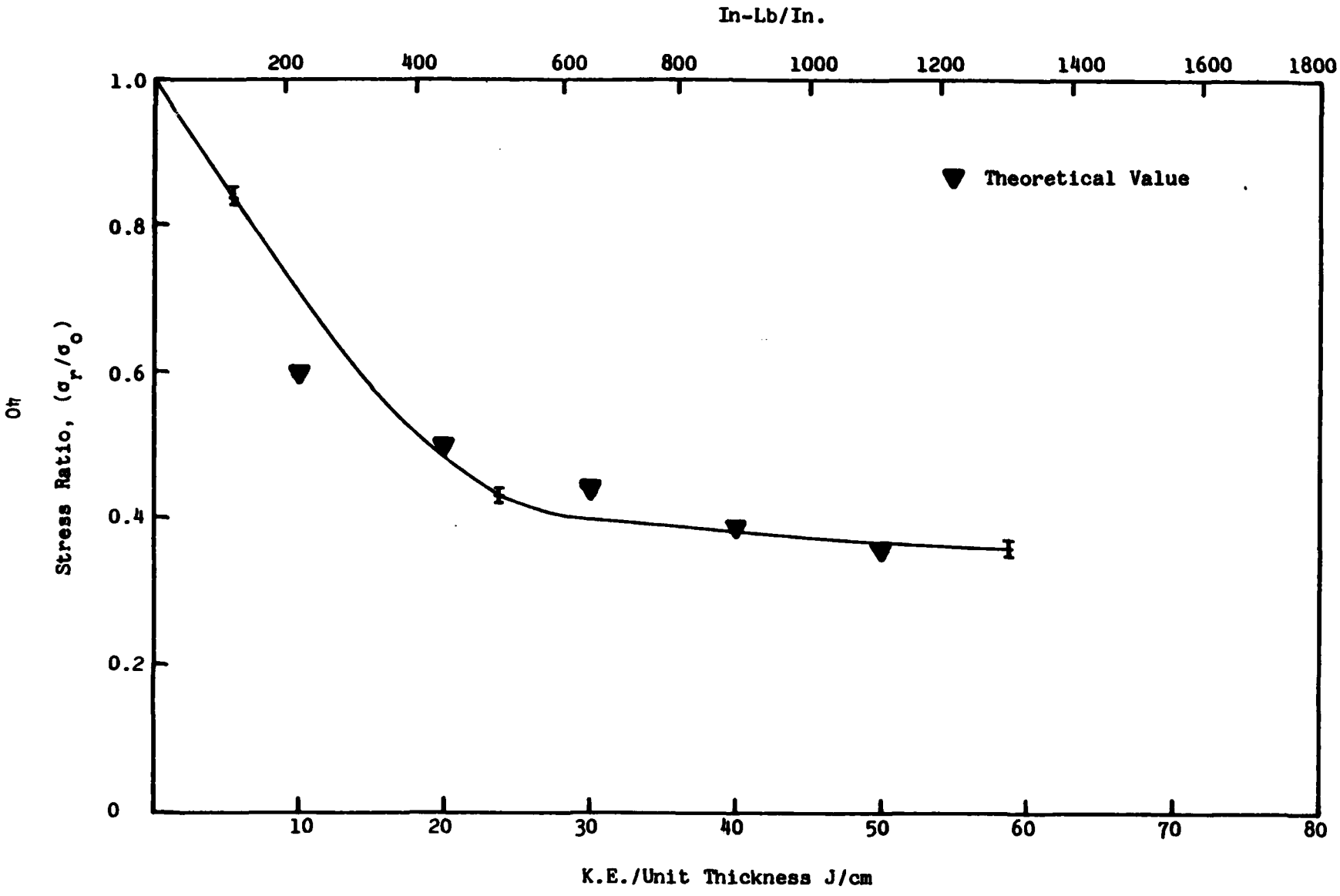

Figure 11. Normalized Residual Stress vs. K.E. of Projectile: Compression.

Impact Test With Pre-Load (Scatter Study):

This test was performed in compression at three velocities as in tension tests to study the residual strength and the catastrophic failure scatter. The results are tabulated in Table IX and the values of (σ/σ_o) with respect to K.E./unit thickness are plotted as shown in Figure 12. For the purpose of comparison, the faired curve drawn in Figure 10 is shown again in Figure 12. All the specimens impacted at a pre-stress below the faired curve survived and those impacted at a pre-stress above the faired curve failed catastrophically, which means that the faired curve gives a true representation of the failure threshold of these laminates. The scatter of residual stress points was high at an average energy of 5.6 J/cm (125.9 in-lb/in). At energies of 24.4 J/cm (549 in-lb/in) and 56.8 J/cm (1277 in-lb/in), the residual stress points were in the vicinity of the faired curve. Residual strength scatter in compression tests was found to be less compared to the scatter in tension tests.

Fracture Modes

In this section, the photographs of several specimens exhibiting the fracture modes under various test conditions discussed earlier are shown.

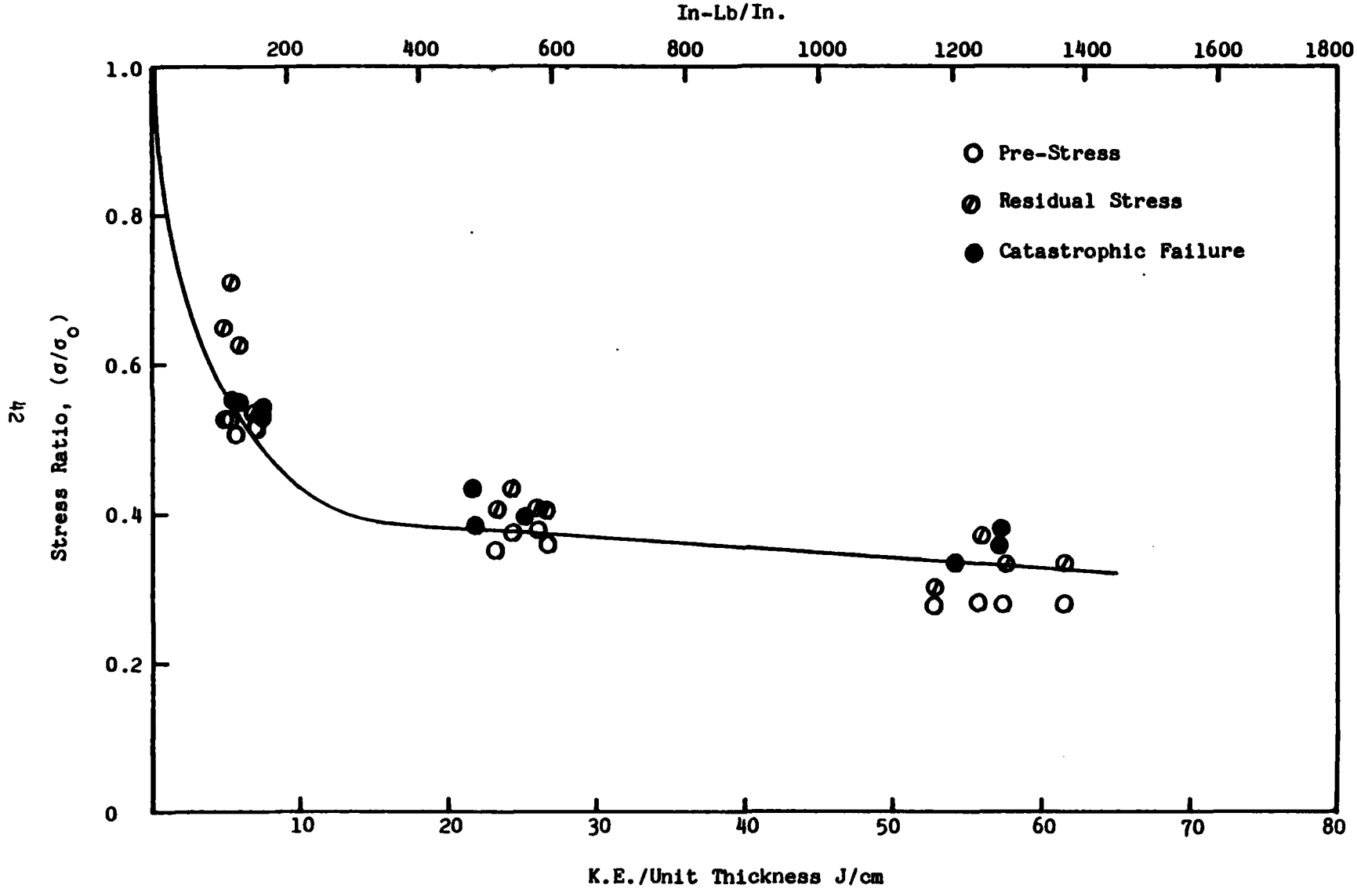

Figure 12. Scatter Study: Compression

Figure 13 shows the failure of a tension sample tested for ultimate strength. The delamination of plies can be clearly seen on both faces of the specimen. On the front face, delamination of plies with ±45, 0 and 90 degree orientation is evident. On the rear face, the same type of laminate failure may also be seen. At higher loads, the fibers started breaking and the complete fracture occurred upon reaching the ultimate load.

The impact damage of a pre-loaded tension test specimen with catastrophic failure upon impact is shown in Figure 14. The impact energy absorbed by this specimen was 9.7 J/cm (217.3 in-lb/in) at a pre-stress of 54% of the ultimate stress. The fibers at the impact zone have broken and a crack has propagated across the width of the specimen due to the combination of the pre-load and the projectile impact. The damage at the area of impact is visible on the front face and the fracture line may be seen on the rear face.

In Figure 15, the damage of a specimen impacted without any pre-load and tested for the post-impact residual strength is shown. Impact energy absorbed by this specimen was 23.2 J/cm (520.4 in-lb/in). The projectile impact has apparently caused the delamination on both the faces and may have initiated a crack. The post-impact tensile load applied to the specimen may have

Front

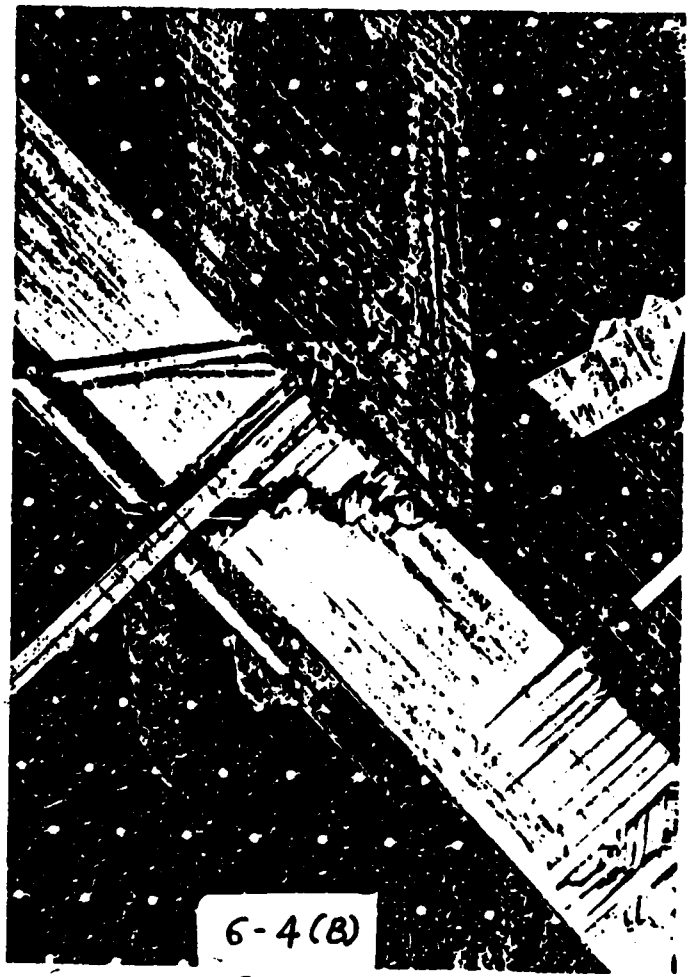

Rear

Figure 13. Fracture due to ultimate tensile stress.

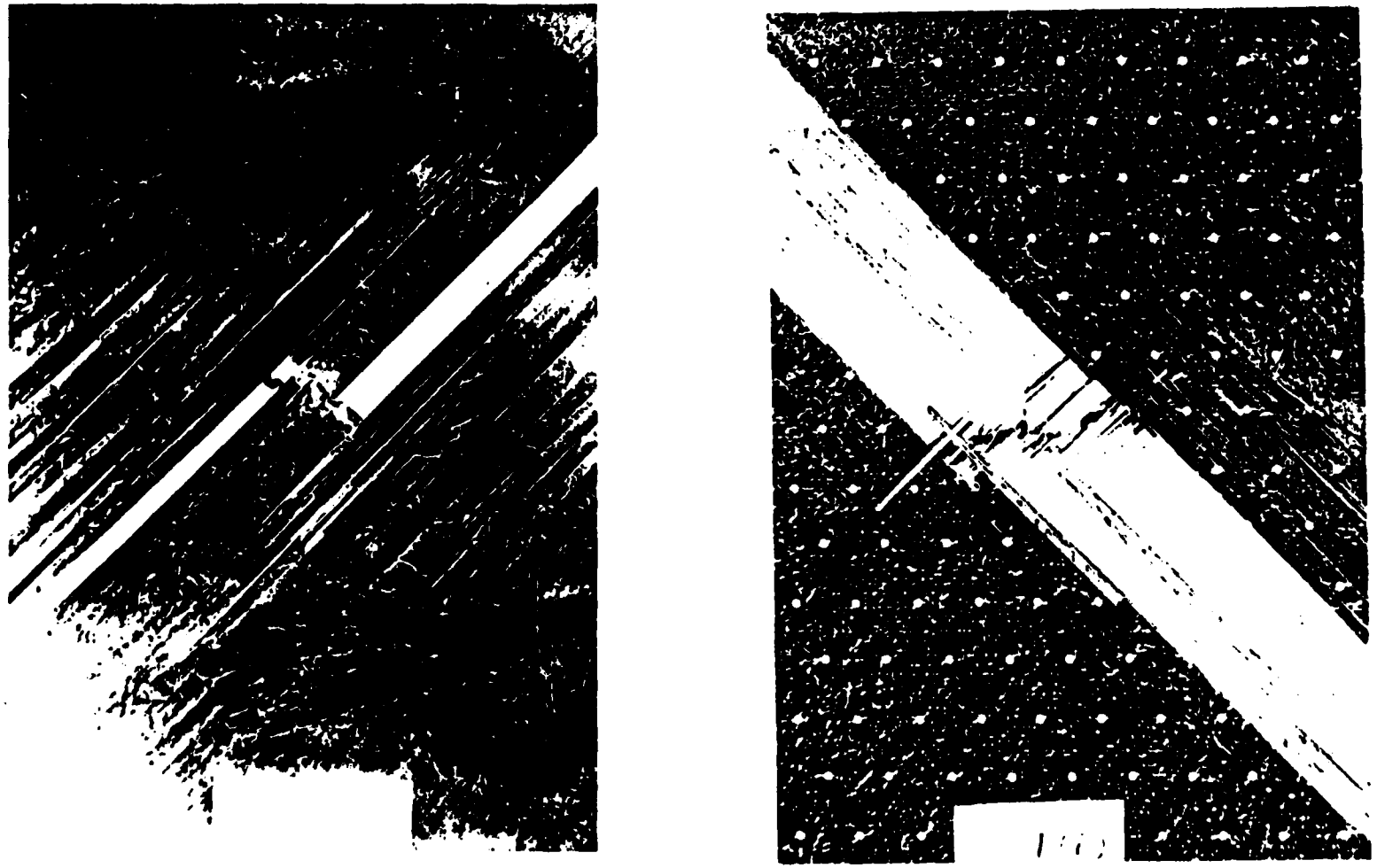

Front

Rear

Figure 14. Catastrophic failure of tension pre-loaded specimen.

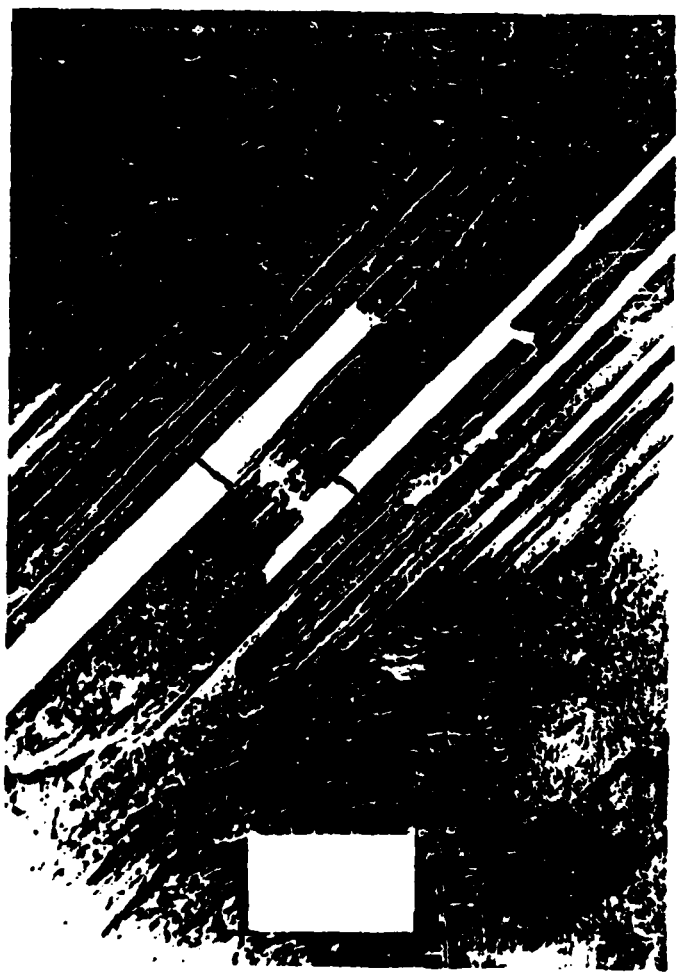

Front

Rear

Figure 15. Fracture of tension specimen with no pre-load.

propagated the crack further resulting in the fracture propagation across the width of the specimen.

The extent of the damage with complete penetration of projectile through a pre-loaded tension test specimen is shown in Figure 16. An impact energy of 46.6 J/cm (1047.4 in/in) was applied to the specimen which was pre-stressed to 33% of the ultimate stress. At penetration, it was noted that there was not much delamination and the specimen survived. Upon continuation of the loading, the delamination and the breaking of fibers occurred resulting in complete fracture near the impact area which may be seen on the rear face of the specimen. The residual stress was 62% of the ultimate stress.

In Figure 17, the failure of a typical compression test specimen loaded to obtain the ultimate strength is shown. The delamination of the plies and the fiber breakage may be seen in the figure. Unlike in the tension test, the fracture did not occur at the center of the specimen. It occurred near one of the tabs.

The photographs of a specimen that failed catastrophically upon impact while under compressive pre-load is shown in Figure 18. The impact energy absorbed by the specimen was 9.8 J/cm (220.9 in-lb/in) at a pre-stress of 52% of the ultimate load. Gross deliminations of plies is not apparent as in the tension tests, but the specimen

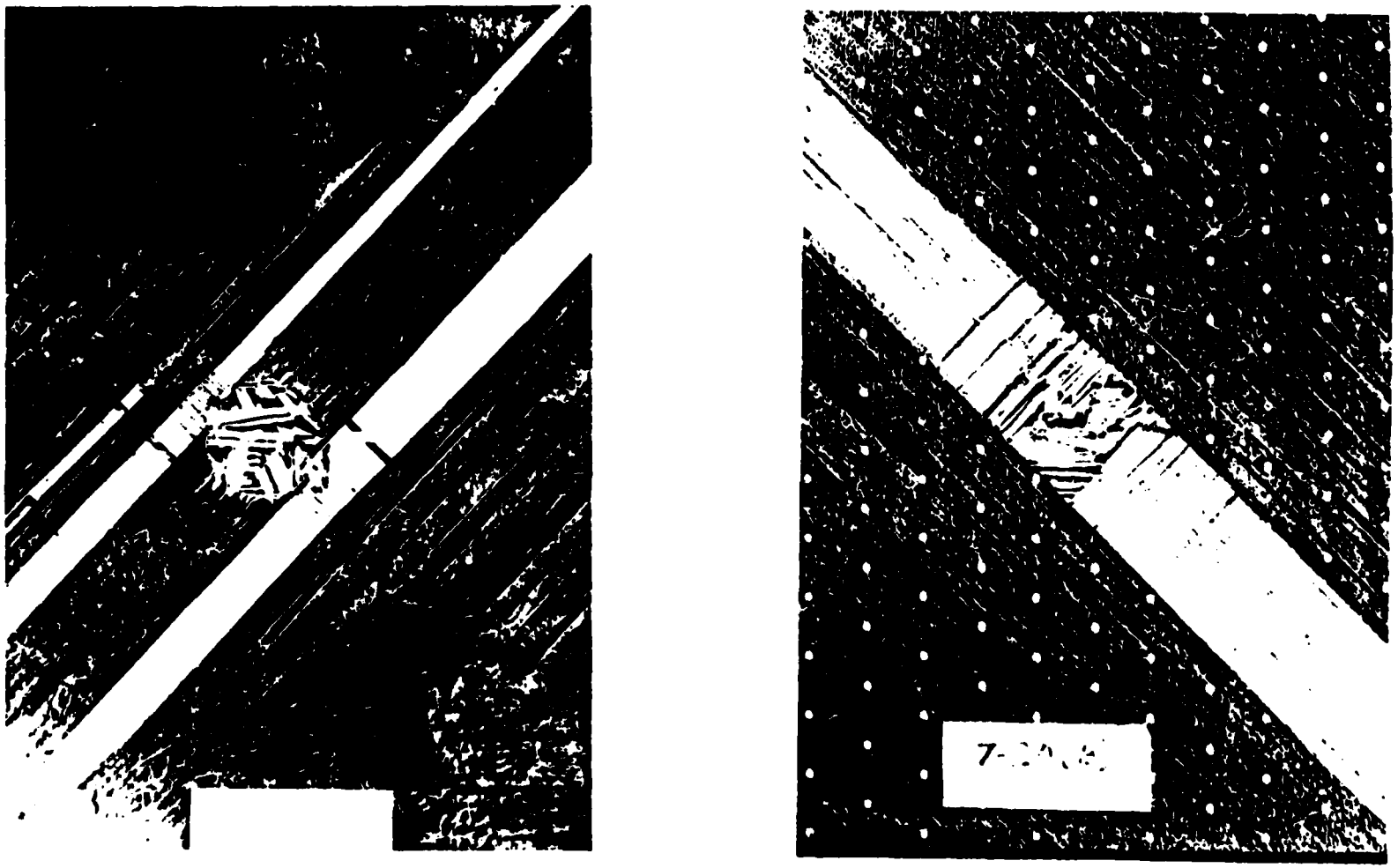

Front

Rear

Figure 16: Pre-loaded tension specimen with complete penetration.

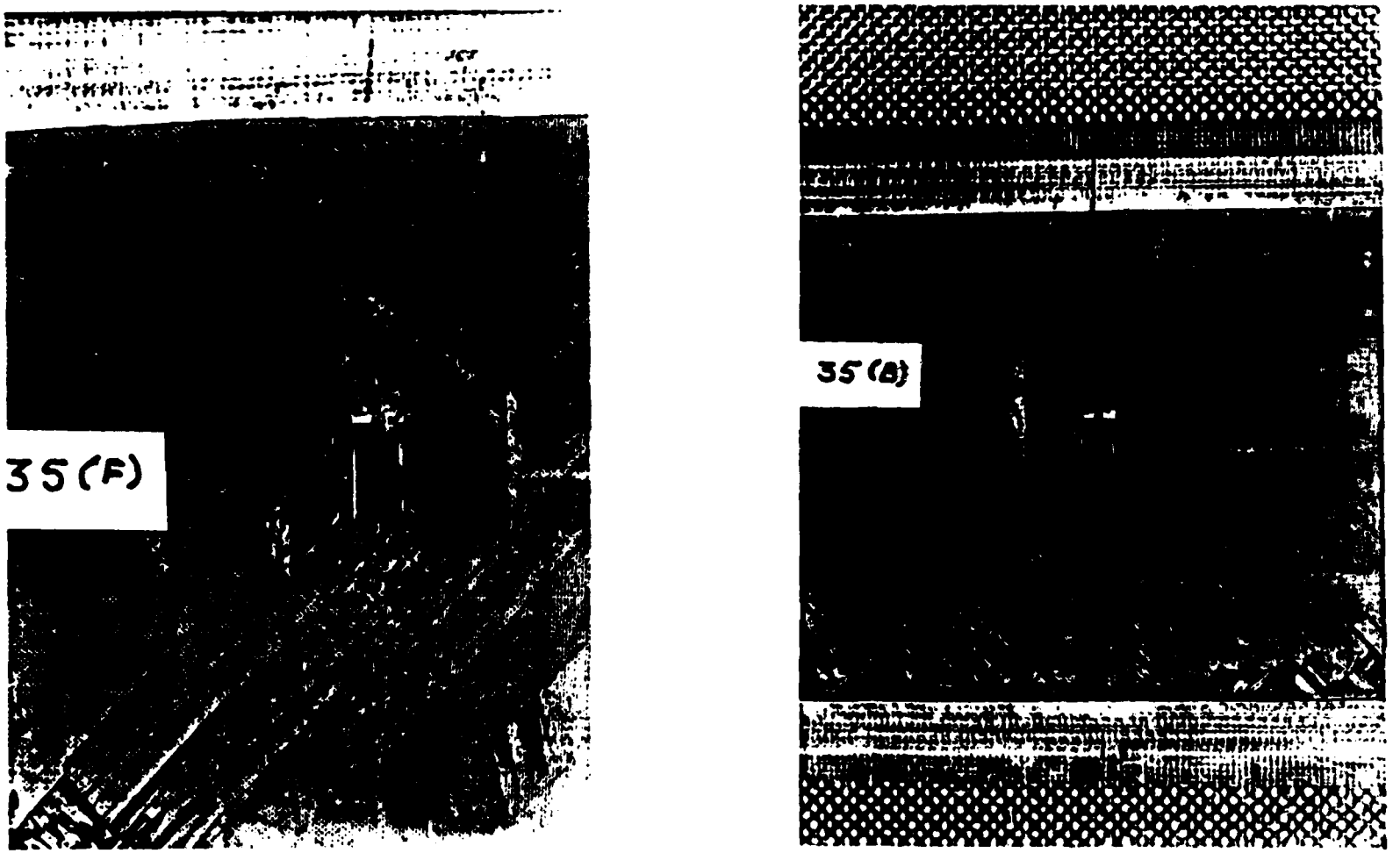

Front

Rear

Figure 17. Fracture due to ultimate compressive stress.

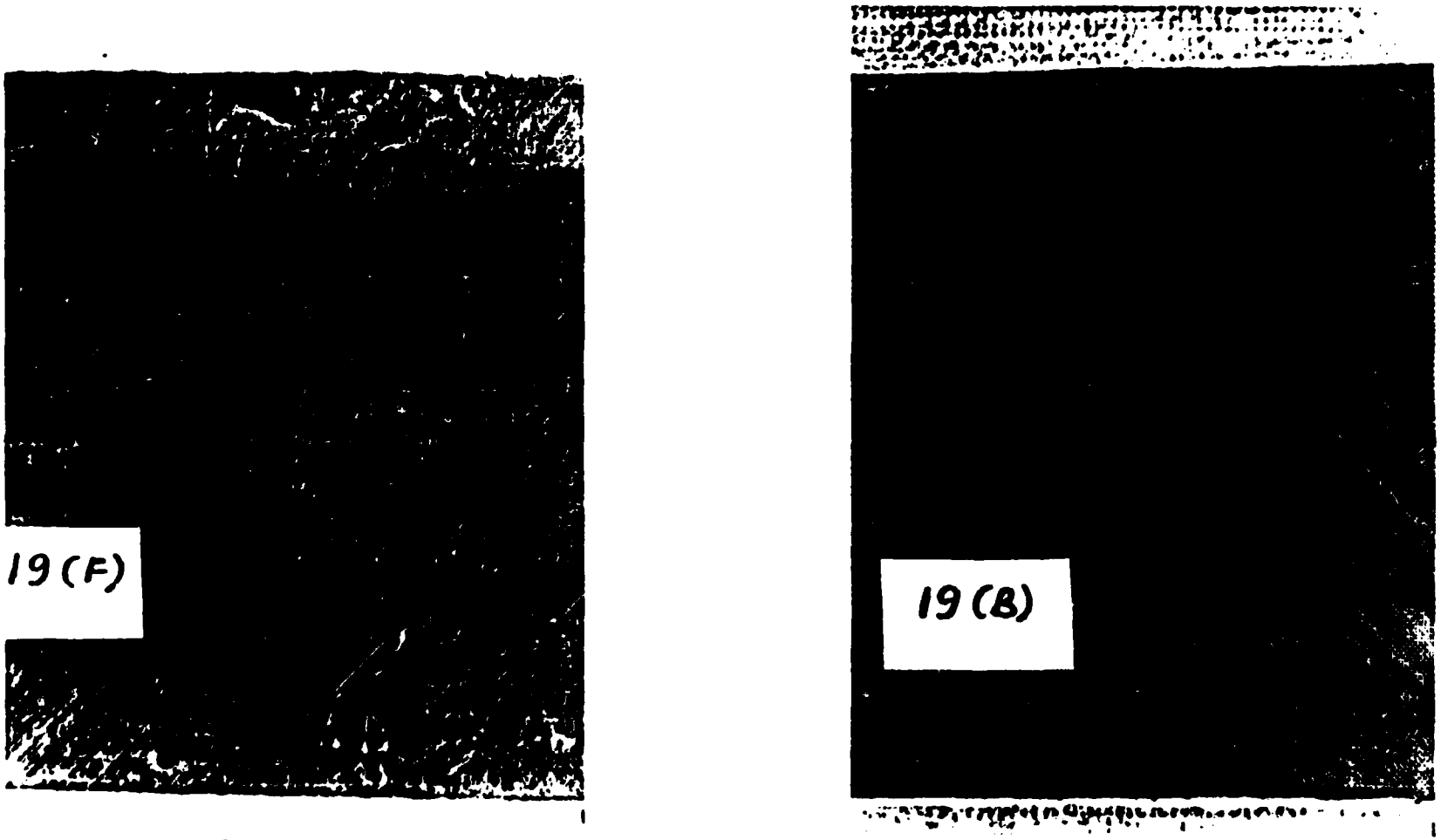

Figure 18. Catastrophic failure of compression pre-loaded specimen.

fractured at the impact zone.

The impact damage in a compression test specimen without pre-load is shown in Figure 19. An impact energy of 24.6 J/cm (554.1 in-lb/in) has apparently caused the visible indentation on the front face and the delamination in the rear face of the specimen. The post-impact residual stress of this specimen was 40% of the ultimate.

The impact damage with complete penetration of the projectile in a pre-loaded specimen under compression is shown in Figure 20. An impact energy of 49.8 J/cm (1119.5 in-lb/in) was applied to the specimen which was pre-stressed to 30% of the ultimate. The specimen failed catastrophically upon impact. Delamination on the front face may be seen to be very little when compared to that on the rear face.

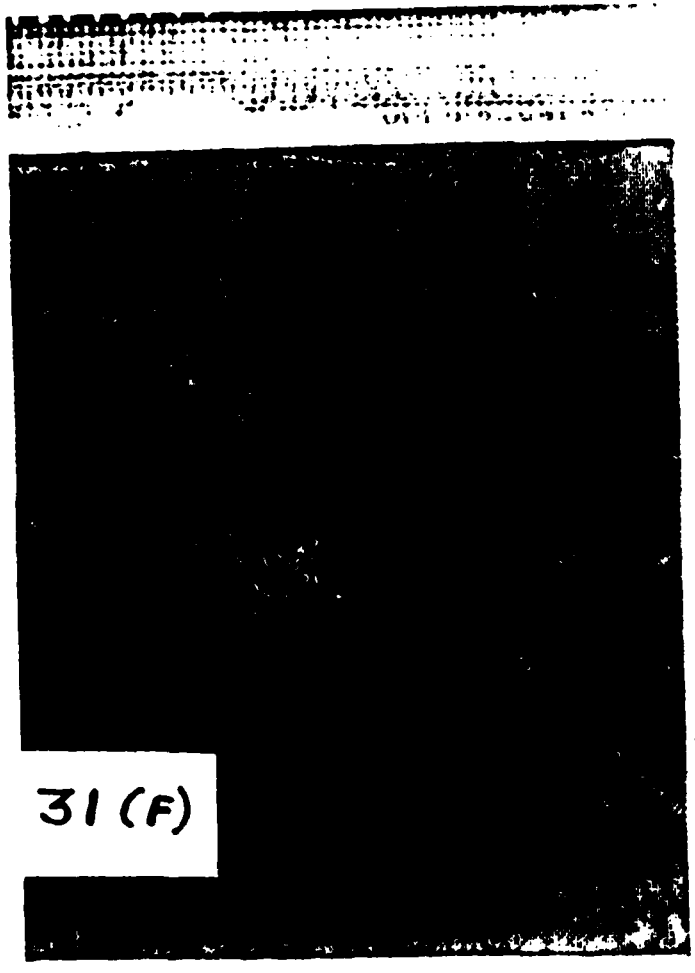

Front

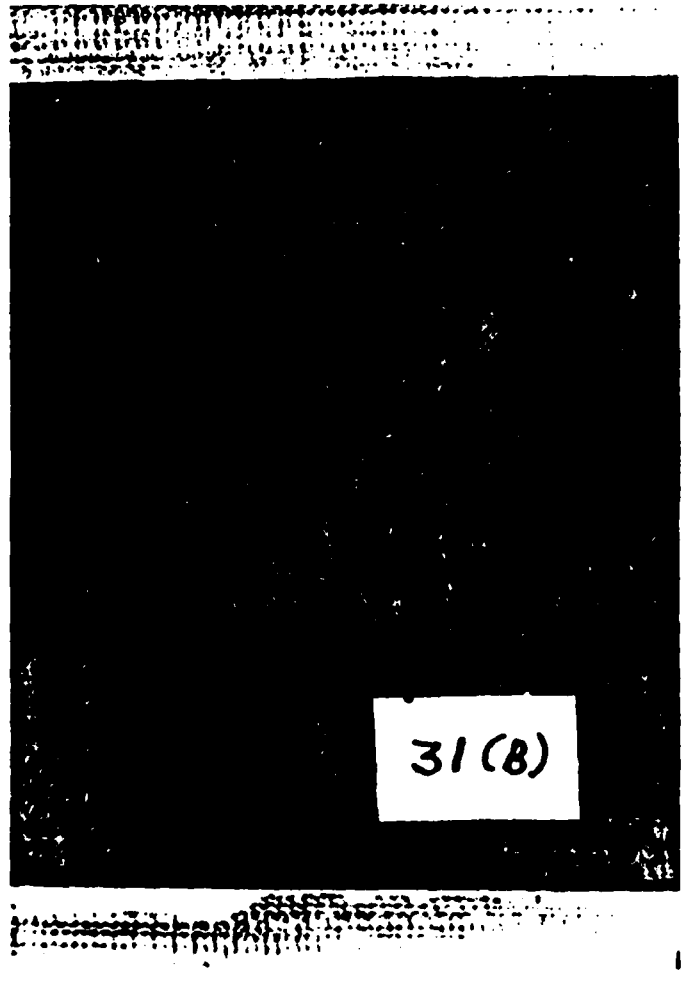

Rear

Figure 19. Fracture of compression specimen with no pre-load.

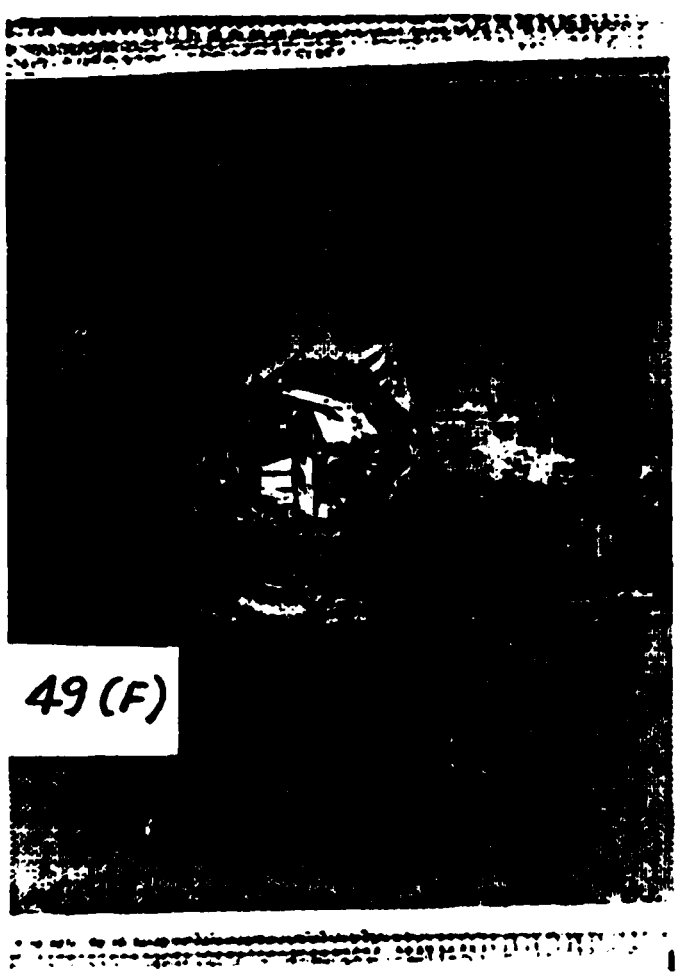

Front

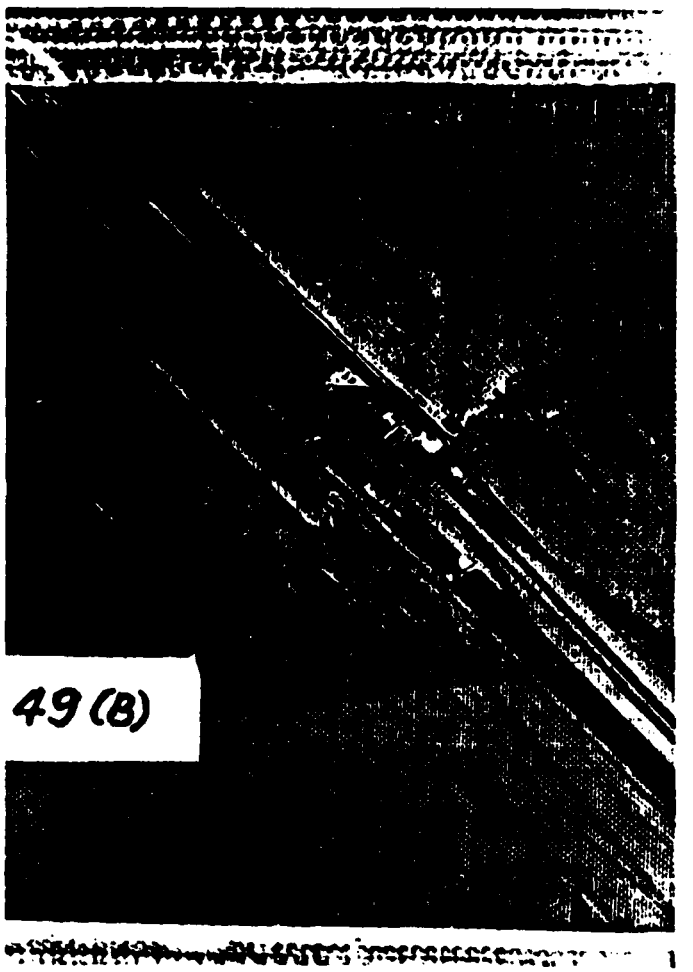

Rear

Figure 20. Pre-loaded compression specimen with complete penetration.

SECTION VII

CONCLUSIONS

The residual strength of the composite materials subjected to projectile impact while under the tensile and the compressive loads can be predicted using the analytical model as presented in this report. The linear regression analysis is adopted for calculating some constants that appear in the analytical model. The analytical method was applied to various loading situations in the laminated composite materials. The analytically calculated values show good agreement with the experimental values in all cases. This model may be adopted in predicting the residual strength of impact-damaged composite materials having different orientations, laminate stacking sequences, etc. However, before one could apply the model, some of the material constants will have to be determined by performing tests on a few specimens for each laminate orientation and stacking sequence.

The combination of the tensile pre-load and the impact at velocities close to penetration causes a high strength degradation of up to 71% compared to a reduction of 43% in the post impact residual strength values without any pre-load. In compression tests, at impact velocities nearer to the penetration velocity, the strength degradation of laminates subjected to impact

with pre-load and without pre-load is asymptotic (Figures 10 and 11). The total strength degradation with pre-load followed by impact is 68% and without pre-load it is 65%. Therefore, it may be stated that the pre-load causes significant reduction in the residual strength of tension-loaded laminates, but not in the compression loaded laminates. However, in the compression loaded laminates, at lower velocities, where the strength reduction values with pre-load and without pre-load are not asymptotic, the difference in residual strength is considerable (Figures 10 and 11).

The post-impact residual stress scatter of pre-loaded specimens in tension and compression was found to be high at low impact energy and low at high impact energy. The scatter in compression was lower compared to scatter in tension for corresponding impact energy levels.

REFERENCES

1. Waddoups, M.E., Eisenmann, J.R., Kaminski, B.E., "Macroscopic Fracture Mechanics of Advanced Composite Materials," Journal of Composite Materials, Vol. 5, October, 1971, pp. 446-454.

2. Whitney, J.M. and Nuismer, R.J., "Stress Fracture Criteria for Laminated Composites Containing Stress Concentrations," Journal of Composite Materials, Vol. 8, 1974, pp. 253-265.

3. Nuismer, R.J. and Whitney, J.M., "Uniaxial Failure of Composite Laminates Containing Stress Concentrations," Fracture Mechanics of Composites, STP 593, ASTM, Philadelphia, 1975, pp. 117-142.

4. Yeow, Y.T., Morris, D.H. and Brinson, H.F., "A Correlative Study Between Analysis and Experiment on the Fracture Behavior of Graphite/Epoxy Composites," Journal of Testing and Evaluation, JTEVA, Vol. 7, No. 2, March 1979, pp. 117-125.

5. Husman, G.E., Whitney, J.m. and Halpin, J.C., "Residual Strength Characterization of Laminated Composites Subjected to Impact Loading," Foreign Object Impact Damage to Composites, STP 568, ASTM 1975, pp. 92-113.

6. Awerbuch, Jonathan and Hahn, Thomas H., "Hard Object Impact Damage of Metal Matrix Composites," Journal of Composite Materials, Vol. 10, July 1976, pp. 231-257.

7. Sharma, A.V., "Low Velocity Impact Tests on Fibrous Composite Sandwich Structures," Test Methods and Design Allowables for Fibrous Composites, STP 734, C.C. Chamis edition, ASTM, 1981, pp. 54-70.

8. Sharma, A.V., "Design and Testing of Small Composite Specimens," Final Report prepared for Langley Research Center, NASA, December, 1981.

9. Whitney, J.M., Private Communication.

APPENDIX A

TABLES

TABLE I. Panel Data (Average Values)

Specimen	Resin Content % by Weight	Specific Gravity	Fiber Vol. % by Weight	Nominal Voids Content %
Tension	32.3	1.57	60.6	-0.6
Compression	28.2	1.57	64.8	0.9

Table II: Ultimate Tensile Stress - Strain Data

Specimen No.	Laminate Thickness t cm. in.	Area A cm^2 in^2	Ultimate Load P kN kips	Ultimate Stress σ_o GPa ksi	Ultimate Strain ε
4-8	0.229 0.090	1.742 0.270	67.4 15.2	387.1 56.2	0.008
6-4	0.226 0.089	1.723 0.267	72.6 16.3	421.2 61.1	0.010
6-3	0.224 0.088	1.710 0.265	71.4 16.0	417.3 60.5	0.009
7-17	0.218 0.086	1.671 0.259	65.8 14.8	394.0 57.1	0.008
1-20	0.221 0.087	1.677 0.260	64.8 14.6	386.4 56.0	0.008
2-6	0.224 0.088	1.703 0.264	65.3 14.7	383.4 55.6	0.009

Table III: Experimental Data - Tension (Pre-Loaded Specimens)

Specimen No.	Pre-Load P_i kN / kips	Stress At Impact σ_i GPa / ksi	Residual Load P_r kN / kips	Residual Stress σ_r GPa / ksi	Stress Ratio $\frac{\sigma_i}{\sigma_o}$	Stress Ratio $\frac{\sigma_r}{\sigma_o}$	Projectile Velocity Forward m/sec / ft/sec	Projectile Velocity Rebound m/sec / ft/sec	Net K.E. joule / in-lb.	Laminate Thickness t cm / in	Net K.E./t joule/cm / in-lb/in
2-13	40.0 9.0	232.4 33.7	51.9 13.5	347.8 50.5	0.58	0.87	18.6 61.0	3.4 11.2	0.5 4.6	0.226 0.089	2.3 50.9
1-6	40.5 9.1	237.8 34.5	*	237.8 34.5	0.60	0.60	23.8 78.0	2.7 9.0	0.9 7.6	0.224 0.088	3.8 85.9
7-6	37.8 8.5	226.3 32.8	62.9 14.1	376.5 54.6	0.57	0.95	24.4 80.0	5.5 18.0	0.9 7.7	0.218 0.086	4.0 89.0
1-15	27.1 6.1	166.0 24.1	67.0 15.1	384.4 55.8	0.42	0.95	25.3 83.0	4.3 14.0	1.0 8.4	0.229 0.090	4.2 93.7
A-5	58.3 13.1	311.5 45.2	66.2 14.9	354.0 51.4	0.78	0.89	26.2 86.0	3.4 11.0	1.0 9.1	0.246 0.097	4.5 94.6
6-16	50.1 11.3	292.9 42.5	*	292.9 42.5	0.74	0.74	26.2 86.0	3.4 11.0	1.0 9.1	0.224 0.088	4.6 104.2
4-6	39.1 8.8	224.7 32.6	46.1 10.4	264.9 38.4	0.56	0.67	26.5 87.0	3.4 11.0	1.1 9.4	0.229 0.090	4.6 104.3
4-19	40.3 9.1	229.4 33.3	41.1 9.3	234.5 34.0	0.58	0.59	28.0 92.0	5.5 18.0	1.2 10.3	0.231 0.091	5.0 112.7
4-20	46.3 10.4	259.8 37.7	*	259.8 37.7	0.65	0.65	28.4 93.0	4.9 16.0	1.2 10.6	0.234 0.092	5.0 115.2

*Catastrophic failure upon impact

Table III (Continued)

Specimen No.	Pre-Load P_i kN kips	Stress At Impact σ_i GPa ksi	Residual Load P_r kN kips	Residual Stress σ_r GPa ksi	Stress Ratio $\frac{\sigma_i}{\sigma_o}$	Stress Ratio $\frac{\sigma_r}{\sigma_o}$	Projectile Velocity Forward m/sec ft/sec	Projectile Velocity Rebound m/sec ft/sec	Net K.E. joule in-lb.	Laminate Thickness t cm in	Net K.E./t joule/cm in-lb/in
3-10	43.4 9.8	258.6 37.5	*	258.6 37.5	0.65	0.65	28.7 94.0	4.9 16.0	1.2 10.8	0.218 0.086	5.6 125.8
2-17	40.0 9.0	224.0 32.5	*	224.0 32.5	0.56	0.56	29.0 95.0	2.7 9.0	1.3 11.3	0.234 0.092	5.4 122.5
5-5	37.8 8.5	227.1 33.0	43.2 9.7	259.8 37.7	0.57	0.65	32.9 108.0	6.7 22.0	1.6 14.0	0.218 0.086	7.3 163.8
4-4	38.7 8.7	227.2 33.0	*	227.2 33.0	0.57	0.57	35.4 116	5.2 16.9	1.9 16.6	0.224 0.088	8.4 188.6
7-19	36.0 8.1	215.6 31.3	61.0 13.7	365.2 53.0	0.54	0.92	36.9 121.0	7.9 26.0	2.0 17.6	0.218 0.086	9.1 204.6
1-7	35.6 8.0	208.9 30.3	*	208.9 30.3	0.53	0.53	38.1 125.0	4.0 13.2	2.2 19.4	0.224 0.088	9.8 221.3
2-4	37.8 8.5	214.7 31.1	*	214.7 31.1	0.54	0.54	38.4 126.0	4.2 13.6	2.2 19.8	0.231 0.091	9.7 217.3
5-19	38.7 8.7	229.8 33.3	*	229.8 33.3	0.58	0.58	40.2 132.0	7.3 24.0	2.4 21.2	0.221 0.087	10.9 244.2
1-5	39.1 8.8	227.0 32.9	*	227.0 32.9	0.57	0.57	40.5 133.0	4.7 15.4	2.5 22.0	0.226 0.089	11.0 247.1

*Catastrophic failure upon impact

Table III (Continued)

Specimen No.	Pre-Load P_i kN kips	Stress At Impact σ_i GPa ksi	Residual Load P_r kN kips	Residual Stress σ_r GPa ksi	Stress Ratio $\frac{\sigma_i}{\sigma_o}$	$\frac{\sigma_r}{\sigma_o}$	Projectile Velocity Forward m/sec ft/sec	Rebound m/sec ft/sec	Net K.E. joule in-lb.	Laminate Thickness t cm in	Net K.E./t joule/cm in-lb/in
5-11	44.9 10.1	275.3 39.9	*	275.3 39.9	0.69	0.69	40.8 134.0	8.5 28.0	2.5 21.6	0.213 0.084	11.5 256.7
2-9	39.1 8.8	228.1 33.1	*	228.1 33.1	0.57	0.57	41.2 135.0	5.9 19.3	2.5 22.6	0.226 0.089	11.2 252.7
4-10	37.4 8.4	216.1 31.3	*	216.1 31.3	0.54	0.54	42.7 140.0	8.5 28.0	2.7 23.8	0.226 0.089	11.9 266.4
4-21	27.0 6.1	155.3 22.5	40.2 9.0	230.6 33.5	0.39	0.58	48.5 159.0	4.1 13.4	3.6 31.7	0.229 0.090	15.6 351.5
4-13	24.7 5.6	138.9 20.2	43.9 9.9	246.7 35.8	0.35	0.62	49.1 161.0	4.3 14.0	3.7 32.4	0.234 0.092	15.7 352.3
4-11	37.8 8.5	219.5 31.8	*	219.5 31.8	0.55	0.55	48.8 160.0	6.6 21.8	3.6 31.7	0.226 0.089	15.8 355.7
2-11	37.8 8.5	218.7 31.7	*	218.7 31.7	0.55	0.55	54.0 177.0	4.0 13.0	4.5 39.5	0.226 0.089	19.7 443.5
5-13	24.7 5.6	160.8 23.3	38.6 8.7	251.5 36.5	0.40	0.63	57.0 187.0	3.7 12.0	5.0 43.9	0.201 0.079	24.7 555.5
1-2	18.0 4.1	104.2 15.1	40.0 9.0	231.5 33.6	0.26	0.60	59.4 195.0	9.1 30.0	5.3 46.8	0.226 0.089	23.4 523.8

*Catastrophic failure upon impact

Table III (Continued)

Specimen No.	Pre-Load P_i kN kips	Stress At Impact σ_i GPa ksi	Residual Load P_r kN kips	Residual Stress σ_r GPa ksi	Stress $\frac{\sigma_i}{\sigma_o}$	Ratio $\frac{\sigma_r}{\sigma_o}$	Projectile Velocity Forward m/sec ft/sec	Rebound m/sec ft/sec	Net K.E. joule in-lb.	Laminate Thickness t cm in	Net K.E./t joule/cm in-lb/in
5-18	18.1 4.1	105.8 15.3	42.5 9.6	248.3 36.0	0.27	0.62	61.0 200.0	6.7 22.0	5.6 49.8	0.224 0.088	25.1 565.8
7-7	18.1 4.1	104.8 15.2	54.1 12.2	313.0 45.4	0.26	0.79	61.0 200.0	6.7 22.0	5.6 49.8	0.226 0.089	24.9 559.4
6-24	24.7 5.6	145.8 21.1	45.0 10.2	265.2 38.5	0.37	0.67	64.9 213.0	4.1 13.4	6.4 57.0	0.221 0.087	29.1 654.5
6-6	27.7 6.2	153.4 22.3	34.8 7.8	192.5 27.9	0.39	0.48	66.8 219.0	7.7 25.3	6.7 59.6	0.236 0.093	28.6 641.2
3-5	29.7 6.7	175.1 25.4	*	175.1 25.4	0.44	0.44	67.1 220.0	2.9 9.5	6.9 60.8	0.211 0.087	31.1 699.7
6-22	18.5 4.2	106.0 15.4	42.2 9.5	242.0 35.1	0.27	0.61	64.7 212.0	7.0 23.0	6.3 55.9	0.229 0.090	27.6 621.8
1-3	27.5 6.2	163.3 23.7	*	163.3 23.7	0.41	0.41	71.3 234.0	5.5 18.0	7.8 68.6	0.221 0.087	35.1 788.3
7-8	21.4 4.8	123.0 17.8	40.6 9.1	234.1 34.0	0.31	0.59	78.6 258.0	4.3 14.0	9.5 83.6	0.221 0.087	42.8 961.2
2-15	21.4 4.8	122.6 17.8	*	122.6 17.8	0.31	0.31	79.3 260.0	4.3 14.0	9.6 84.9	0.229 0.090	41.9 943.7

*Catastrophic failure upon impact

Table III (Continued)

Specimen No.	Pre-Load P_i kN / kips	Stress At Impact σ_i GPa / ksi	Residual Load P_r kN / kips	Residual Stress σ_r GPa / ksi	Stress $\frac{\sigma_i}{\sigma_o}$	Ratio $\frac{\sigma_r}{\sigma_o}$	Projectile Forward m/sec / ft/sec	Velocity Rebound m/sec / ft/sec	Net K.E. joule / in-lb.	Laminate Thickness t cm / in	Net K.E./t joule/cm / in-lb/in
1-9	24.4 5.5	142.4 20.7	*	142.4 20.7	0.36	0.36	85.0 279.0	3.4 11.0	11.1 98.0	0.226 0.089	49.0 1102.1
7-4	18.5 4.2	109.6 15.9	37.6 8.5	223.3 32.4	0.28	0.57	88.4 290.0	**	12.0 106.0	0.221 0.087	54.2 1218.0
5-14	22.3 5.0	132.1 19.2	*	132.1 19.2	0.33	0.33	96.0 315.0	**	14.1 125.0	0.221 0.087	63.9 1437.0
6-7	17.9 4.0	103.7 15.0	33.7 7.6	194.9 28.3	0.26	0.49	96.9 318.0	**	14.4 127.4	0.226 0.089	63.7 1431.6
3-9	20.7 4.7	121.0 17.6	*	121.0 17.6	0.30	0.30	99.7 327.0	**	15.2 134.8	0.224 0.088	68.0 1531.1
4-7	20.9 4.7	118.7 17.2	23.6 5.3	133.8 19.4	0.30	0.34	100.3 329.0	**	15.4 136.4	0.231 0.091	66.7 1498.7
7-20	22.8 5.1	131.0 19.0	42.9 9.7	246.5 35.8	0.33	0.62	82.9 272.0	**	10.5 93.2	0.226 0.089	46.6 1047.4
4-1	16.5 3.7	102.0 14.8	28.0 6.3	173.8 25.2	0.26	0.44	80.8 265.0	9.5 31.0	9.9 87.2	0.211 0.083	46.7 1051.4
2-2	17.8 4.0	96.7 14.0	24.7 5.6	134.3 19.5	0.24	0.34	106.7 350.0	**	17.4 154.3	0.241 0.095	72.4 1624.8

*Catastrophic failure upon impact
**Complete penetration

Table III (continued)

Specimen No.	Pre-Load P_i kN kips	Stress At Impact σ_i GPa ksi	Residual Load P_r kN kips	Residual Stress σ_r GPa ksi	Stress Ratio $\frac{\sigma_i}{\sigma_o}$	$\frac{\sigma_r}{\sigma_o}$	Projectile Velocity Forward m/sec ft/sec	Rebound m/sec ft/sec	Net K.E. joule in-lb.	Laminate Thickness t cm in	Net K.E./t joule/cm in-lb/in
6-1	13.3 3.0	82.7 12.0	28.1 6.3	169.2 24.5	0.21	0.43	106.7 350.0	**	17.4 154.3	0.211 0.083	82.7 1860.0

**Complete penetration

Table IV: Experimental Data - Tension (No Pre-Load)

Specimen No.	Residual Load P_r kN kips	Residual Stress σ_r GPa ksi	Stress Ratio $\frac{\sigma_r}{\sigma_o}$	Projectile Velocity Forward m/sec ft/sec	Projectile Velocity Rebound m/sec ft/sec	Net K.E. joule in-lb	Laminate Thickness t cm in	Net K.E./t joule/cm in-lb/in
7-5	64.5 14.5	381.2 55.3	0.96	29.9 98.0	3.7 12.0	1.4 11.9	0.218 0.086	6.2 138.6
2-3	61.8 13.9	349.7 50.7	0.88	29.3 96.0	4.0 13.0	1.3 11.4	0.231 0.091	5.6 125.3
4-14	60.9 13.7	351.3 51.0	0.88	34.1 112.0	4.9 16.0	1.8 15.5	0.226 0.089	5.7 174.0
1-16	56.0 12.6	324.4 47.1	0.82	31.7 104.0	4.9 16.0	1.5 13.3	0.226 0.089	6.6 149.5
1-8	67.2 15.1	390.2 56.6	0.98	27.1 89.0	2.7 9.0	1.1 9.9	0.226 0.089	5.0 111.0
7-3	74.7 13.8	367.6 53.3	0.92	39.6 130.0	5.5 18.0	2.4 20.9	0.218 0.086	10.8 242.9
7-21	68.9 15.5	412.0 59.8	1.04	29.6 97.0	3.4 11.0	1.3 11.7	0.218 0.086	4.5 136
A-8	68.9 15.5	394.7 57.3	0.99	22.0 72.0	2.1 7.0	0.7 6.5	0.229 0.090	3.2 71.9
2-1	60.9 13.7	352.6 51.1	0.89	29.0 95.0	4.0 13.0	1.3 11.2	0.226 0.089	4.1 125.4

Table IV (Continued)

Specimen No.	Residual Load P_r kN kips	Residual Stress σ_r GPa ksi	Stress Ratio $\frac{\sigma_r}{\sigma_o}$	Projectile Velocity Forward m/sec ft/sec	Rebound m/sec ft/sec	Net K.E. joule in-lb	Laminate Thickness t cm in	Net K.E./t joule/cm in-lb/in
1-18	48.0 10.8	276.6 40.1	0.70	33.8 111.0	4.6 15.0	1.7 15.2	0.229 0.090	7.5 169.3
3-1	60.9 13.7	329.4 47.8	0.83	32.6 107.0	4.3 14.0	1.6 14.2	0.241 0.095	4.9 149.3
1-12	57.8 13.0	346.9 50.3	0.87	31.1 102.0	4.6 15.0	1.5 12.8	0.218 0.086	4.9 149.2
A-1	44.5 10.0	245.1 35.6	0.62	60.7 199.0	7.6 25.0	5.6 49.1	0.236 0.093	23.5 528.0
1-1	45.8 10.3	285.5 41.4	0.72	59.1 194.0	7.3 24.0	5.3 46.7	0.211 0.083	25.1 562.6
4-5	46.7 10.5	268.7 39.0	0.68	57.3 188.0	7.3 24.0	5.0 43.8	0.226 0.089	21.9 492.2
6-14	46.3 10.4	273.5 39.7	0.69	61.3 201.0	7.3 24.0	5.7 50.2	0.221 0.087	25.7 576.8
2-14	52.5 11.8	300.6 43.6	0.76	48.8 160.0	6.7 22.0	3.6 31.7	0.229 0.090	15.7 351.6
4-12	47.6 10.7	272.9 39.6	0.69	53.6 176.0	6.1 20.0	4.4 38.5	0.229 0.090	19.0 428.1

Table IV (Continued)

Specimen No.	Residual Load P_r kN kips	Residual Stress σ_r GPa ksi	Stress Ratio $\frac{\sigma_r}{\sigma_o}$	Projectile Velocity Forward m/sec ft/sec	Rebound m/sec ft/sec	Net K.E. joule in-lb	Laminate Thickness t cm in	Net K.E./t joule/cm in-lb/in
6-11	45.4 10.2	253.6 36.8	0.64	59.7 196.0	7.6 25.0	5.4 47.6	0.229 0.090	23.5 529.1
1-19	41.8 9.2	246.8 35.8	0.62	57.9 190.0	7.3 24.0	5.1 44.8	0.218 0.086	23.2 520.4
6-17	43.6 9.8	249.2 36.1	0.63	64.6 212.0	7.6 25.0	6.3 55.8	0.229 0.090	27.6 620.5
3-2	32.9 7.4	178.7 25.9	0.45	86.9 285.0	14.3 47.0	11.3 99.6	0.239 0.094	47.1 1059.1
7-2	47.2 10.6	282.0 40.9	0.71	89.0 292.0	**	12.1 107.4	0.218 0.086	55.7 1249.2
4-2	38.7 8.7	216.8 31.4	0.54	91.4 300.0	**	12.8 113.4	0.234 0.092	54.8 1232.6
2-12	29.8 6.7	175.2 25.4	0.44	89.0 292.0	**	12.6 111.1	0.224 0.088	56.2 1262.8
7-12	46.3 10.4	276.9 40.2	0.70	92.7 304.0	**	13.2 116.4	0.218 0.086	60.3 1354.0
A-6	38.3 8.6	198.8 28.8	0.50	96.0 315.0	**	14.1 125.0	0.252 0.099	56.2 1262.9

**Complete penetration

Table IV (Continued)

Specimen No.	Residual Load P_r kN kips	Residual Stress σ_r GPa ksi	Stress Ratio $\frac{\sigma_r}{\sigma_o}$	Projectile Velocity Forward m/sec ft/sec	Projectile Velocity Rebound m/sec ft/sec	Net K.E. joule in-lb	Laminate Thickness t cm in	Net K.E./t joule/cm in-lb/in
5-6	34.7 7.8	203.2 29.5	0.51	89.6 294.0	**	12.3 108.9	0.224 0.088	55.1 1237.6
7-14	45.4 10.2	271.2 39.3	0.68	86.9 285.0	**	11.6 102.3	0.218 0.086	52.9 1190.0
3-3	31.1 7.0	171.0 24.8	0.43	91.4 300.0	**	12.8 113.4	0.239 0.094	53.7 1206.4

**Complete penetration

Table V: Pre-Load Impact Test - Tension (Scatter Study)

Specimen No.	Pre-Load P_i kN kips	Stress At Impact σ_i GPa ksi	Residual Load P_r kN kips	Residual Stress σ_r GPa ksi	Stress Ratio $\frac{\sigma_i}{\sigma_o}$	Stress Ratio $\frac{\sigma_r}{\sigma_o}$	Projectile Velocity Forward m/sec ft/sec	Projectile Velocity Rebound m/sec ft/sec	Net K.E. joule in-lb.	Laminate Thickness t cm in	Net K.E./t joule/cm in-lb/in
4-16	39.1 8.8	225.7 32.7	*	225.7 32.7	0.57	0.57	33.8 111.0	3.2 10.4	1.7 15.4	0.229 0.090	7.4 171.1
6-21	37.8 8.5	228.9 33.2	48.5 10.9	294.7 42.8	0.58	0.74	30.8 101.0	5.0 16.4	1.4 12.5	0.216 0.085	6.5 147.1
7-16	38.3 8.6	230.3 33.4	63.2 14.2	381.2 55.3	0.58	0.96	30.2 99.0	2.7 8.8	1.4 12.3	0.216 0.085	6.5 144.7
7-13	38.3 8.6	227.6 33.0	63.2 14.2	377.9 54.8	0.57	0.95	27.7 91.0	5.8 19.0	1.1 10.0	0.218 0.086	5.1 116.3
7-11	39.1 8.8	239.7 34.8	64.5 14.5	396.0 57.4	0.60	0.99	30.5 100.0	6.3 20.8	1.4 12.1	0.213 0.084	6.6 144.1
7-18	40.0 9.0	234.2 34.0	66.3 14.9	386.9 56.1	0.59	0.97	31.1 102.0	6.6 21.6	1.4 12.5	0.224 0.088	6.3 142.1
5-7	40.5 9.1	233.7 33.9	54.7 12.3	317.2 46.0	0.59	0.80	28.0 92.0	5.8 19.0	1.2 10.2	0.226 0.089	5.3 114.6
5-4	42.3 9.5	254.3 36.9	*	254.3 36.9	0.64	0.64	28.0 92.0	5.0 16.4	1.2 10.3	0.218 0.086	5.5 119.8
4-3	40.9 9.2	245.9 35.7	*	245.9 35.7	0.62	0.62	29.3 96.0	3.4 11.2	1.3 11.5	0.218 0.086	6.0 133.7

*Catastrophic failure at impact

Table V (Continued)

Specimen No.	Pre-Load P_i kN / kips	Stress At Impact σ_i GPa / ksi	Residual Load P_r kN / kips	Residual Stress σ_r GPa / ksi	Stress Ratio $\frac{\sigma_i}{\sigma_o}$	Stress Ratio $\frac{\sigma_r}{\sigma_o}$	Projectile Velocity Forward m/sec / ft/sec	Projectile Velocity Rebound m/sec / ft/sec	Net K.E. joule / in-lb.	Laminate Thickness t cm / in	Net K.E./t joule/cm / in-lb/in
5-1	40.0 9.0	264.1 38.3	*	264.1 38.3	0.66	0.66	31.1 100.0	4.4 14.5	1.4 12.3	0.198 0.078	7.1 157.7
1-10	39.1 8.8	229.8 33.3	*	229.8 33.3	0.58	0.58	29.4 96.0	5.3 17.4	1.3 11.2	0.224 0.088	5.8 127.3
A-3	37.8 8.5	196.7 28.5	43.2 9.7	224.0 32.5	0.49	0.56	32.6 107.0	5.9 19.3	1.6 14.0	0.252 0.099	6.4 141.4
2-8	35.6 8.0	204.8 29.7	*	204.8 29.7	0.51	0.51	60.1 197.0	10.6 34.7	5.4 47.4	0.229 0.090	23.6 526.7
3-8	31.6 7.1	181.6 26.3	*	181.6 26.3	0.46	0.46	58.8 193.0	7.3 24.0	5.2 46.2	0.226 0.089	23.0 519.1
4-15	26.7 6.0	154.3 22.4	*	154.3 22.4	0.39	0.39	62.2 204.0	7.3 23.8	5.8 57.7	0.229 0.090	25.3 641.1
5-9	26.7 6.0	157.9 22.9	*	157.9 22.9	0.40	0.40	63.4 208.0	5.5 18.0	6.1 54.1	0.224 0.088	27.2 614.8
1-4	24.5 5.5	142.1 20.6	30.7 6.9	179.5 26.0	0.36	0.45	60.4 198.0	6.8 22.3	5.5 48.8	0.226 0.089	24.3 548.3
6-20	25.4 5.7	150.2 21.8	37.8 8.5	224.0 32.5	0.38	0.56	57.6 189.0	7.9 25.8	5.0 44.2	0.221 0.087	22.6 508.1

*Catastrophic failure at impact

Table V (Continued)

Specimen No.	Pre-Load P_i kN kips	Stress At Impact σ_i GPa ksi	Residual Load P_r kN kips	Residual Stress σ_r GPa ksi	Stress Ratio $\frac{\sigma_i}{\sigma_o}$	Stress Ratio $\frac{\sigma_r}{\sigma_o}$	Projectile Velocity Forward m/sec ft/sec	Projectile Velocity Rebound m/sec ft/sec	Net K.E. joule in-lb.	Laminate Thickness t cm in	Net K.E./t joule/cm in-lb/in
3-7	25.4 5.7	134.7 19.5	28.9 6.5	154.5 22.4	0.34	0.39	63.7 209.0	6.3 20.8	6.2 54.5	0.246 0.097	25.2 561.9
6-2	27.1 6.1	158.1 22.9	35.1 7.9	206.6 30.0	0.40	0.52	64.6 212.0	9.7 31.7	6.3 55.4	0.224 0.088	28.1 629.5
2-10	27.6 6.2	156.9 22.8	*	156.9 22.8	0.39	0.39	65.8 216.0	8.8 28.8	6.5 57.7	0.231 0.091	28.1 634.1
1-14	27.6 6.2	167.7 24.3	*	167.7 24.3	0.42	0.42	62.2 204.0	7.3 23.8	5.8 51.7	0.216 0.085	26.9 608.2
2-5	27.1 6.1	148.3 21.5	*	148.3 21.5	0.37	0.37	57.9 190.0	4.3 14.1	5.1 45.2	0.241 0.095	21.2 475.8
1-13	27.6 6.2	163.1 23.7	*	163.1 23.7	0.41	0.41	52.2 191.0	8.2 26.8	5.1 45.1	0.221 0.087	23.1 518.4
2-18	21.8 4.9	124.9 18.1	*	124.9 18.1	0.31	0.31	88.7 291.0	**	12.1 106.7	0.229 0.090	52.8 1185.6
1-11	20.0 4.5	122.6 17.8	26.2 5.9	159.3 23.1	0.31	0.40	88.7 291.0	**	12.1 106.7	0.213 0.084	56.8 1270
4-17	21.8 4.9	124.5 18.1	23.6 5.3	133.9 19.4	0.31	0.34	95.7 314.0	**	14.0 124.2	0.231 0.091	60.6 1364.8

*Catastrophic failure upon impact
**Complete penetration

Table V (Continued)

Specimen No.	Pre-Load P_i kN / kips	Stress At Impact σ_i GPa / ksi	Residual Load P_r kN / kips	Residual Stress σ_r GPa / ksi	Stress Ratio $\frac{\sigma_i}{\sigma_o}$	Stress Ratio $\frac{\sigma_r}{\sigma_o}$	Projectile Velocity Forward m/sec / ft/sec	Projectile Velocity Rebound m/sec / ft/sec	Net K.E. joule / in-lb.	Laminate Thickness t cm / in	Net K.E./t joule/cm / in-lb/in
6-10	20.0 4.5	115.4 16.7	28.5 6.4	163.8 23.8	0.29	0.41	92.1 302.0	**	13.0 114.9	0.229 0.090	56.8 1276.7
5-10	97.0 5.0	132.6 19.2	*	132.6 19.2	0.33	0.33	92.4 303.0	**	13.1 115.7	0.221 0.087	59.3 1329.9
2-7	24.5 5.5	141.7 20.6	*	141.7 20.6	0.36	0.36	89.3 293.0	**	12.2 108.2	0.229 0.090	53.3 1202.2

*Catastrophic failure upon impact
**Complete penetration

Table VI: Ultimate Compressive Stress-Strain Data

Specimen No.	Laminate Thickness t cm. in.	Area A_2 cm^2 in^2	Ultimate Load P kN kips	Ultimate Stress σ_o GPa ksi	Ultimate Strain ε
35	0.221 0.087	1.710 0.265	56.0 12.6	328.2 47.6	0.006
68	0.224 0.088	1.703 0.264	50.3 11.3	295.1 42.8	0.006
64	0.224 0.088	1.703 0.264	54.3 12.2	318.5 46.2	0.006
99	0.224 0.088	1.684 0.261	49.4 11.1	293.0 42.5	0.006
28	0.221 0.087	1.677 0.260	51.6 11.6	307.5 44.6	0.006

Table VII: Experimental Data - Compression (Pre-Loaded Specimens)

Specimen No.	Pre-Load P_i kN / kips	Stress At Impact σ_i GPa / ksi	Residual Load P_r kN / kips	Residual Stress σ_r GPa / ksi	Stress Ratio $\frac{\sigma_i}{\sigma_o}$	Stress Ratio $\frac{\sigma_r}{\sigma_o}$	Projectile Velocity Forward m/sec / ft/sec	Projectile Velocity Rebound m/sec / ft/sec	Net K.E. joule / in-lb	Laminate Thickness t cm / in	Net K.E./t joule/cm / in-lb/in
77	44.5 10.0	261.3 37.9	*	261.3 37.9	0.85	0.85	17.7 58.0	7.6 24.8	0.4 3.4	0.224 0.088	1.7 38.6
17	24.5 5.5	148.2 21.5	48.0 10.8	291.0 42.2	0.48	0.94	20.7 68.0	6.8 22.3	0.6 5.2	0.218 0.086	2.7 60.5
115	31.1 7.0	186.2 27.0	38.3 8.6	228.9 33.2	0.60	0.74	20.7 68.0	3.2 10.4	0.7 5.8	0.218 0.086	3.0 67.4
9	31.6 7.1	188.9 27.4	53.8 12.1	319.2 46.3	0.27	1.03	21.0 69.0	6.8 22.3	0.6 5.4	0.221 0.087	2.8 62.1
13	28.5 6.4	173.1 25.1	50.7 11.4	308.2 44.7	0.56	1.00	23.0 75.4	5.5 17.9	0.8 6.8	0.216 0.085	3.6 80 0
11	24.5 5.5	147.6 21.4	39.1 8.8	235.8 34.2	0.48	0.76	24.4 80.0	6.3 20.8	0.9 7.6	0.218 0.086	3.9 88.4
44	44.0 9.9	255.8 37.1	*	255.8 37.1	0.83	0.83	25.6 84.0	2.7 8.9	1.0 8.8	0.226 0.089	4.4 98.9
18	40.0 9.0	243.4 35.3	*	243.4 35.3	0.79	0.79	25.6 84.0	2.7 8.9	1.0 8.8	0.216 0.085	4.6 103.5
93	31.1 7.0	181.3 26.3	46.3 10.4	269.6 39.1	0.59	0.87	25.6 84.0	6.3 20.8	1.0 8.4	0.226 0.089	4.2 94.4

*Catastrophic failure upon impact

Table VII (Continued)

Specimen No.	Pre-Load P_i kN kips	Stress At Impact σ_i GPa ksi	Residual Load P_r kN kips	Residual Stress σ_r GPa ksi	Stress Ratio $\frac{\sigma_i}{\sigma_o}$	Stress Ratio $\frac{\sigma_r}{\sigma_o}$	Projectile Velocity Forward m/sec ft/sec	Projectile Velocity Rebound m/sec ft/sec	Net K.E. joule in-lb	Laminate Thickness t cm in	Net K.E./t joule/cm in-lb/in
46	35.6 8.0	208.9 30.3	*	208.9 30.3	0.68	0.68	34.4 113.0	4.1 13.4	1.8 15.8	0.224 0.088	8.0 179.5
109	35.6 8.0	223.4 32.4	*	223.4 32.4	0.72	0.72	36.0 118.0	6.3 20.8	1.8 16.0	0.208 0.082	8.7 195.1
19	26.7 6.0	160.7 23.3	*	160.7 23.3	0.52	0.52	38.1 125.0	6.8 22.3	2.1 19.0	0.218 0.086	9.8 220.9
4	24.5 5.5	145.5 21.1	48.9 11.0	291.0 42.2	0.47	0.94	38.4 126.0	5.5 17.9	2.2 19.6	0.221 0.087	10.0 225.3
5	23.1 5.2	144.8 21.0	23.6 5.3	147.6 21.4	0.47	0.48	38.7 127.0	5.0 16.4	2.3 20.0	0.211 0.083	10.7 241.0
121	20.0 4.5	122.0 17.7	21.4 4.8	129.6 18.8	0.40	0.42	42.4 139.0	10.0 32.7	2.6 23.0	0.216 0.085	12.0 270.6
22	27.6 6.2	165.5 24.0	*	165.5 24.0	0.54	0.54	42.4 139.0	8.2 26.8	2.6 23.4	0.218 0.086	12.1 272.1
124	16.0 3.6	97.2 14.1	21.4 4.8	122.0 17.7	0.32	0.40	43.3 142.0	5.5 17.9	2.8 25.0	0.216 0.085	13.1 294.1
62	31.3 7.0	184.8 26.8	*	184.8 26.8	0.60	0.60	43.9 144.0	7.3 23.8	2.9 25.4	0.221 0.087	13.0 292.0

*Catastrophic failure upon impact

Table VII (Continued)

Specimen No.	Pre-Load P_i kN / kips	Stress At Impact σ_i GPa / ksi	Residual Load P_r kN / kips	Residual Stress σ_r GPa / ksi	Stress Ratio $\frac{\sigma_i}{\sigma_o}$	Stress Ratio $\frac{\sigma_r}{\sigma_o}$	Projectile Velocity Forward m/sec / ft/sec	Projectile Velocity Rebound m/sec / ft/sec	Net K.E. joule / in-lb	Laminate Thickness t cm / in	Net K.E./t joule/cm / in-lb/in
32	26.7 6.0	162.0 23.5	*	162.0 23.5	0.53	0.53	45.1 148.0	15.4 50.6	2.8 24.4	0.216 0.085	12.8 287.1
71	18.7 4.2	107.6 15.6	24.9 5.6	142.7 20.7	0.35	0.46	46.9 154.0	7.7 25.3	3.3 29.0	0.229 0.090	14.3 322.2
73	18.7 4.2	107.6 15.6	20.9 4.7	120.0 17.4	0.35	0.39	47.5 156.0	9.1 29.8	4.5 39.6	0.229 0.090	19.9 440.0
84	15.1 3.4	89.6 13.0	22.2 5.0	132.4 19.2	0.29	0.43	49.7 163.0	8.6 28.3	3.7 32.5	0.221 0.087	16.6 373.6
2	18.7 4.2	120.0 17.4	*	120.0 17.4	0.39	0.39	51.8 170.0	7.7 25.3	4.0 35.6	0.206 0.081	19.5 439.5
51	15.6 3.5	91.0 13.2	22.2 5.0	129.6 18.8	0.30	0.42	52.7 173.0	10.0 32.7	4.1 36.4	0.226 0.089	18.2 408.6
27	20.0 4.5	122.0 17.7	*	122.0 17.7	0.40	0.40	53.3 175.0	12.1 39.7	4.1 36.6	0.216 0.085	19.1 430.6
7	20.5 4.6	124.1 18.0	*	124.1 18.0	0.40	0.40	56.4 185.0	12.7 41.7	4.6 41.0	0.216 0.085	21.4 482.4
21	15.6 3.5	9.38 13.6	23.1 5.2	139.3 20.2	0.30	0.45	61.0 200.0	11.9 39.0	5.5 48.4	0.218 0.086	25.1 562.8

*Catastrophic failure upon impact

Table VII (Continued)

Specimen No.	Pre-Load P_i kN / kips	Stress At Impact σ_i GPa / ksi	Residual Load P_r kN / kips	Residual Stress σ_r GPa / ksi	Stress Ratio $\frac{\sigma_i}{\sigma_o}$	Stress Ratio $\frac{\sigma_r}{\sigma_o}$	Projectile Velocity Forward m/sec / ft/sec	Projectile Velocity Rebound m/sec / ft/sec	Net K.E. joule / in-lb	Laminate Thickness t cm / in	Net K.E./t joule/cm / in-lb/in
39	16.0 3.6	94.5 13.7	20.9 4.7	123.4 17.9	0.31	0.40	69.2 227.0	11.6 38.0	7.1 63.2	0.224 0.088	31.9 718.2
10	18.7 4.2	111.0 16.1	20.0 4.5	118.6 17.2	0.36	0.38	71.6 235.0	11.9 39.0	7.6 67.6	0.221 0.087	34.6 777.0
29	16.9 3.8	101.4 14.7	19.1 4.3	115.1 16.7	0.33	0.37	72.5 238.0	12.3 40.2	7.8 69.4	0.218 0.086	36.0 807.0
92	20.0 4.5	116.5 16.9	20.9 4.7	121.3 17.6	0.38	0.39	75.0 246.0	12.9 42.2	8.6 76.2	0.226 0.089	38.1 856.2
72	19.1 4.3	109.6 15.9	*	109.6 15.9	0.36	0.36	80.0 262.0	**	9.8 86.4	0.229 0.090	42.6 960.0
78	16.9 3.8	97.9 14.2	*	97.9 14.2	0.32	0.32	82.6 271.0	**	10.5 92.6	0.226 0.089	46.3 1040.4
79	14.2 3.2	83.4 12.1	19.6 4.4	115.1 16.7	0.27	0.37	82.6 271.0	**	10.5 92.6	0.224 0.088	46.9 1052.3
49	15.6 3.5	92.4 13.4	*	92.4 13.4	0.30	0.30	84.7 278.0	**	11.0 97.4	0.221 0.087	49.8 1119.5
52	13.8 3.1	82.0 11.9	19.6 4.4	116.5 16.9	0.27	0.38	85.8 281.5	**	11.3 99.8	0.221 0.087	51.0 1147.1

*Catastrophic failure upon impact
**Complete penetration

Table VII (Continued)

Specimen No.	Pre-Load P_i kN / kips	Stress At Impact σ_i GPa / ksi	Residual Load P_r kN / kips	Residual Stress σ_r GPa / ksi	Stress Ratio $\frac{\sigma_i}{\sigma_o}$	Stress Ratio $\frac{\sigma_r}{\sigma_o}$	Projectile Velocity Forward m/sec / ft/sec	Projectile Velocity Rebound m/sec / ft/sec	Net K.E. joule / in-lb	Laminate Thickness t cm / in	Net K.E./t joule /cm / in-lb/cm
30	17.3 3.9	105.5 15.3	18.2 4.1	111.0 16.1	0.34	0.36	86.0 282.0	**	11.3 100.2	0.216 0.085	52.4 1178.8
55	16.9 3.8	99.2 14.4	*	99.3 14.4	0.32	0.32	97.2 319.0	**	14.5 128.2	0.223 0.088	65.0 1456.8
53	14.7 3.3	86.2 12.5	18.7 4.2	109.6 15.9	0.28	0.36	95.4 313.0	**	13.9 123.4	0.223 0.088	62.5 1402.3

*Catastrophic failure upon impact
**Complete penetration

Table VIII: Experimental Data - Compression (No Pre-Load)

Specimen No.	Residual Load P_r kN / kips	Residual Stress σ_r GPa / ksi	Stress Ratio $\frac{\sigma_r}{\sigma_o}$	Projectile Velocity Forward m/sec / ft/sec	Projectile Velocity Rebound m/sec / ft/sec	Net K.E. joule / in-lb	Laminate Thickness t cm / in	Net K.E./t joule/cm / in-lb/in
33	45.4	275.8	0.89	29.0	7.7	1.2	0.216	5.5
	10.2	40		95.0	25.3	10.6	0.085	121.7
122	43.6	270.3	0.88	29.3	7.6	1.2	0.211	5.8
	9.8	39.2		96.0	24.8	10.8	0.083	130.1
95	43.1	253.0	0.82	27.1	3.8	1.1	0.224	4.9
	9.7	36.7		89.0	12.4	9.8	0.088	111.4
123	41.8	244.8	0.79	30.2	11.3	1.2	0.224	5.3
	9.4	35.5		99.0	37.2	10.6	0.088	120.5
96	44.9	266.1	0.86	28.4	8.3	1.2	0.226	5.1
	10.1	38.6		93.3	27.3	10.6	0.089	114.6
97	42.3	245.5	0.80	29.7	9.8	1.2	0.226	5.4
	9.5	35.6		97.4	32.2	10.6	0.089	120.2
118	40.0	242.7	0.79	33.2	11.3	1.5	0.216	6.9
	9.0	35.2		109.0	37.2	13.2	0.085	155.3
94	44.9	264.1	0.86	25.1	9.1	0.85	0.224	3.8
	10.1	38.3		82.5	29.8	7.5	0.088	85.2
67	24.5	142.7	0.46	58.8	7.9	5.2	0.221	23.6
	5.5	20.7		193.0	26.0	46.1	0.087	529.9

Table VIII (Continued)

Specimen No.	Residual Load P_r kN kips	Residual Stress σ_r GPa ksi	Stress Ratio $\frac{\sigma_r}{\sigma_o}$	Projectile Velocity Forward m/sec ft/sec	Projectile Velocity Rebound m/sec ft/sec	Net K.E. joule in-lb	Laminate Thickness t cm in	Net K.E./t joule/cm in-lb/in
114	20.5 4.6	124.1 18.0	0.40	64.6 212.0	7.3 24.0	6.3 55.9	0.216 0.085	29.2 657.6
43	23.6 5.3	139.3 20.2	0.45	57.0 187.0	6.7 22.0	4.9 43.5	0.224 0.088	21.9 494.3
102	22.2 5.0	128.9 18.7	0.42	64.3 211.0	13.9 45.6	6.0 53.5	0.226 0.089	26.8 601.1
41	22.7 5.1	134.4 19.5	0.44	59.7 196.0	17.4 57.0	5.0 44.3	0.221 0.087	22.6 509.2
31	20.5 4.6	124.1 18.0	0.40	61.4 201.5	17.4 57.1	5.3 47.1	0.216 0.085	24.6 554.1
38	21.4 4.8	126.2 18.3	0.41	57.9 190.0	12.1 39.7	4.9 43.5	0.224 0.088	21.9 494.3
69	23.6 5.3	139.3 20.2	0.45	57.3 188.0	6.0 19.8	5.0 44.0	0.224 0.088	22.2 500.0
83	24.5 5.5	144.1 20.9	0.47	54.6 179.0	5.8 19.0	4.5 39.9	0.224 0.088	20.1 453.4
60	19.1 4.3	113.8 16.5	0.37	89.3 293.0	**	12.2 108.2	0.221 0.087	55.3 1243.7

**Complete penetration

Table VIII (Continued)

Specimen No.	Residual Load P_r kN / kips	Residual Stress σ_r GPa / ksi	Stress Ratio $\frac{\sigma_r}{\sigma_o}$	Projectile Velocity Forward m/sec / ft/sec	Projectile Velocity Rebound m/sec / ft/sec	Net K.E. joule / in-lb	Laminate Thickness t cm / in	Net K.E./t joule/cm / in-lb/in
34	18.2	106.9	0.35	92.1	**	13.0	0.224	58.0
	4.1	15.5		302.0		114.9	0.088	1305.7
82	19.1	113.1	0.37	90.2	**	12.5	0.224	55.7
	4.3	16.4		296.0		110.4	0.088	1254.6
111	18.7	115.8	0.38	93.3	**	13.3	0.211	63.2
	4.2	16.8		306.0		118.0	0.083	1421.7
37	17.8	104.8	0.34	91.7	**	12.9	0.224	57.6
	4.0	15.2		301.0		114.2	0.088	1297.7
116	19.1	117.9	0.38	89.6	**	12.3	0.213	57.8
	4.3	17.1		294.0		108.9	0.084	1296.4
66	17.8	104.8	0.34	96.0	**	14.1	0.224	63.1
	4.0	15.2		315.0		125.0	0.088	1420.5

**Complete penetration

Table IX: Pre-Load Impact Test - Compression (Scatter Study)

Specimen No.	Pre-Load P_i kN / kips	Stress At Impact σ_i GPa / ksi	Residual Load P_r kN / kips	Residual Stress σ_r GPA / ksi	Stress Ratio $\frac{\sigma_i}{\sigma_o}$	Stress Ratio $\frac{\sigma_r}{\sigma_o}$	Projectile Velocity Forward m/sec / ft/sec	Projectile Velocity Rebound m/sec / ft/sec	Net K.E. joule / in-lb	Laminate Thickness t cm / in	Net K.E./t joule/cm / in-lb/in
3	26.7 6.0	164.8 23.9	35.6 8.0	219.9 31.9	0.53	0.71	27.6 90.4	4.5 14.9	1.1 10.0	0.213 0.084	5.3 119.0
20	27.1 6.1	164.1 23.8	32.9 7.4	199.3 28.9	0.53	0.65	27.1 89.0	4.3 14.0	1.1 9.7	0.218 0.086	5.0 112.8
6	28.0 6.3	168.2 24.4	*	168.2 24.4	0.55	0.55	29.4 96.5	5.7 18.8	1.3 11.3	0.218 0.086	5.9 131.4
12	26.7 6.0	161.3 23.4	27.1 6.1	164.1 23.8	0.52	0.53	32.5 106.7	6.8 22.3	1.6 13.7	0.218 0.086	7.1 159.3
8	27.1 6.1	164.8 23.9	*	164.8 23.9	0.53	0.53	32.8 107.5	7.3 23.8	1.6 13.9	0.216 0.085	7.3 163.5
14	26.7 6.0	158.6 23.0	32.9 7.4	195.8 28.4	0.51	0.63	31.1 102.0	10.0 32.7	1.3 11.8	0.221 0.087	6.0 135.6
88	28.9 6.5	166.2 24.1	*	166.2 24.1	0.54	0.54	33.4 109.7	7.3 23.8	1.6 14.5	0.229 0.090	7.2 161.1
70	29.4 6.6	168.2 24.4	*	168.2 24.4	0.55	0.55	28.8 94.5	6.6 21.8	1.2 10.7	0.229 0.090	5.3 118.9
24	18.2 4.1	108.2 15.7	21.4 4.8	126.9 18.4	0.35	0.41	59.1 194.0	10.1 33.2	5.2 46.0	0.221 0.087	23.5 528.7

*Catastrophic failure upon impact

Table IX (Continued)

Specimen No.	Pre-Load P_i kN / kips	Stress At Impact σ_i GPa / ksi	Residual Load P_r kN / kips	Residual Stress σ_r GPa / ksi	Stress Ratio $\frac{\sigma_i}{\sigma_o}$	Stress Ratio $\frac{\sigma_r}{\sigma_o}$	Projectile Velocity Forward m/sec / ft/sec	Projectile Velocity Rebound m/sec / ft/sec	Net K.E. joule / in-lb	Laminate Thickness t cm / in	Net K.E./t joule/cm / in-lb/in
25	18.7 4.2	112.4 16.3	20.5 4.6	123.4 17.9	0.36	0.40	62.8 206.0	10.7 35.0	5.9 51.9	0.218 0.086	26.9 603.5
91	20.0 4.5	116.5 16.9	*	116.5 16.9	0.38	0.38	57.6 189.0	8.7 28.4	5.0 44.0	0.226 0.089	22.0 494.4
89	20.0 4.5	116.5 16.9	21.8 4.9	126.9 18.4	0.38	0.41	63.3 207.6	12.1 39.7	5.9 52.3	0.226 0.089	26.2 587.6
26	22.2 5.0	134.4 19.5	*	134.4 19.5	0.44	0.44	57.3 188.0	14.1 46.3	4.7 41.8	0.218 0.086	21.7 486.1
87	18.2 4.1	107.6 15.6	21.8 4.9	128.2 18.6	0.35	0.42	62.5 205.0	12.9 42.2	5.7 50.7	0.224 0.088	25.6 576.1
23	20.0 4.5	118.6 17.2	21.8 4.9	129.6 18.8	0.38	0.42	61.3 201.2	15.1 49.6	5.4 47.9	0.221 0.087	24.5 550.6
85	21.4 4.8	124.1 18.0	*	124.1 18.0	0.40	0.40	62.0 203.5	12.1 39.7	5.7 50.2	0.226 0.089	25.1 564.0
76	20.0 4.5	116.5 16.9	*	116.5 16.9	0.38	0.38	91.9 301.6	**	13.0 114.6	0.226 0.089	57.3 1287.6
47	18.7 4.2	109.6 15.9	*	109.6 15.9	0.36	0.36	91.4 300.0	**	12.8 113.4	0.224 0.088	57.2 1288.6

*Catastrophic failure upon impact
**Complete penetration

Table IX (Continued)

Specimen No.	Pre-Load P_i kN kips	Stress At Impact σ_i GPa ksi	Residual Load P_r kN kips	Residual Stress σ_r GPA ksi	Stress Ratio $\frac{\sigma_i}{\sigma_o}$	Stress Ratio $\frac{\sigma_r}{\sigma_o}$	Projectile Velocity Forward m/sec ft/sec	Projectile Velocity Rebound m/sec ft/sec	Net K.E. joule in-lb	Laminate Thickness t cm in	Net K.E./t joule/cm in-lb/in
74	17.8 4.0	102.7 14.9	*	102.7 14.9	0.33	0.33	89.9 295.0	**	12.4 109.7	0.229 0.090	54.1 1218.9
50	14.2 3.2	85.5 12.4	16.9 3.8	101.4 14.7	0.28	0.33	94.5 310.0	**	13.7 121.1	0.221 0.087	61.9 1392.0
81	14.7 3.3	86.2 12.5	15.6 3.5	91.7 13.3	0.28	0.30	88.1 289.0	**	11.9 105.2	0.224 0.088	53.1 1195.5
80	14.7 3.3	86.2 12.5	19.6 4.4	115.1 16.7	0.28	0.37	90.5 297.0	**	12.6 111.1	0.224 0.088	56.0 1262.5
55	15.1 3.4	87.6 12.7	15.1 3.9	100.7 14.6	0.28	0.33	92.4 303.0	**	13.1 115.7	0.226 0.089	57.8 1330.0

APPENDIX B

LINEAR REGRESSION ANALYSIS

a) Tension Test With Pre-Load:

From Figure 7, value of stress ratio σ/σ_o is noted for different values of K.E./unit thickness (x) in J/cm and tabulated as follows:

Sl. No.	x J/cm	$y = (\sigma_o/\sigma_r)^2$	x^2	xy	σ_r/σ_o (Experimental Value)	σ_r/σ_o (Calculated Value)
1	10	4.00	100	40	0.50	0.46
2	20	5.67	400	113.4	0.42	0.41
3	30	7.30	900	219.0	0.37	0.40
4	40	8.65	1600	346.0	0.34	0.35
5	50	9.77	2500	488.5	0.32	0.33
6	60	10.41	3600	624.4	0.31	0.31
7	70	11.11	4900	777.8	0.30	0.30
8	80	11.89	6400	951.3	0.29	0.28
Sum	360	68.80	20400	3560.3		

AD-A122 166 IMPACT-INITIATED DAMAGE IN LAMINATED COMPOSITES(U) 2/2
NORTH CAROLINA AGRICULTURAL AND TECHNICAL STATE UNIV
GREENSBO.. V S AVVA 30 SEP 82 AFOSR-TR-82-1038
UNCLASSIFIED F49620-80-C-0050 F/G 11/4 NL

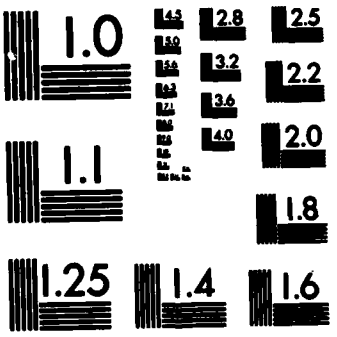

For linear regression

$$\begin{bmatrix} \sum_1^n 1 & \sum_1^n x \\ \sum_1^n x & \sum_1^n x^2 \end{bmatrix} = \begin{bmatrix} \sum_1^n y \\ \sum_1^n (xy) \end{bmatrix}$$

$$\begin{bmatrix} 8 & 360 \\ 360 & 20400 \end{bmatrix} = \begin{bmatrix} 68.8 \\ 3560.3 \end{bmatrix}$$

This can be written in the form of simultaneous equations

$$\begin{aligned} 8b + 360a &= 68.8 \\ 360b + 20400a &= 3560.3 \end{aligned}$$

Solving the above two equations we get

$$a = 0.111$$

$$b = 3.605$$

Linear equation can be written as

$$y = ax + b$$

or $$y = 0.111x + 3.605$$

since $$a = 2K,$$

$$2K = 0.111$$

and $$b = 1-2K\ W_o$$

$$3.605 = 1 - 0.111\ W_o$$

$$W_o = -23.47$$

Using these values of 2K and W_o in equation (5) of Section III (σ/σ_o) is calculated. These calculated values are shown in the table for comparison with experimental values.

b) Tension Test - Without Pre-Load

Sl. No.	x J/cm	$y = (\sigma_o/\sigma_r)^2$	x^2	xy	σ_r/σ_o (Experimental Value)	σ_r/σ_o (Calculated Value)
1	10	1.52	100	15.20	0.81	0.77
2	20	2.16	400	43.25	0.68	0.70
3	30	2.52	900	75.59	0.63	0.65
4	40	2.78	1600	111.11	0.60	0.60
5	50	2.97	2500	148.50	0.58	0.57
Sum	150	11.95	5500	393.65		

two simultaneous equations are:

$$5b + 150a = 11.95$$
$$150b + 5500a = 393.65$$

solving the above equations yields:

$$a = 0.035$$

$$b = 1.34$$

Therefore, $2K = 0.035$

Since, $b = 1-2K\ W_o$

$$1.34 = 1-0.035\ W_o$$

$$W_o = -9.71$$

Using these values of 2K and W_o, (σ_r/σ_o) is calculated and the calculated values are shown in the Table above.

c) Compression Test - With Pre-Load:

Sl. No.	x J/cm	$y = (\sigma_o/\sigma_r)^2$	x^2	xy	σ_r/σ_o (Experimental Value)	σ_r/σ_o (Calculated Value)
1	10	5.17	100	51.7	0.44	0.42
2	20	6.93	400	138.6	0.38	0.40
3	30	7.31	900	219.30	0.37	0.38
4	40	7.72	1600	308.80	0.36	0.36
5	50	8.65	2500	432.50	0.34	0.34
6	60	9.18	3600	550.80	0.33	0.33
Sum	210	44.96	9100	1701.70		

Two simultaneous equations are:

$$6b + 210a = 44.96$$
$$210b + 9100a = 1701.70$$

Solving the above equations yields:

$$a = 0.073$$

$$b = 4.931$$

Therefore, $2K = 0.073$

Since, $b = 1-2K\ W_o$

$$4.931 = 1-0.073\ W_o$$

$$W_o = -53.85$$

Using these values of 2K and W_o, (σ_r/σ_o) is calculated and the calculated values are shown in the Table above.

d) Compression Test - Without Pre-Load:

Sl. No.	x J/cm	$y = (\sigma_o/\sigma_r)^2$	x^2	xy	σ_r/σ_o (Experimental Value)	σ_r/σ_o (Calculated Value)
1	10	2.04	100	20.40	0.70	0.60
2	20	4.34	400	86.80	0.48	0.50
3	30	6.25	900	187.50	0.40	0.44
4	40	6.57	1600	262.80	0.39	0.39
5	50	6.93	2500	346.50	0.38	0.36
Sum	150	26.13	5500	904.00		

Two simultaneous equations are:

$$5b + 150a = 26.13$$
$$150b + 5500a = 904.00$$

Solving the above equations yields:

$$a = 0.120$$

$$b = 1.623$$

Therefore, $2K = 0.120$

Since, $b = 1-2K\ W_o$

$$1.623 = 1-0.120\ W_o$$

$$W_o = -5.192$$

Using these values of 2K and W_o, (σ_r/σ_o) is calculated and the calculated values are shown in the Table above.

APPENDIX C

Calculation of Rebound Velocity of Projectile

Following sample calculation is made to determine the rebound velocity of projectile on tension specimen No. 1-1 photographed and shown in Figure 21.

Frequency of stroboscope light beam used in this case was 250 flashes per second. Three positions of the projectile are seen in first rebound path in the photograph, which means, stroboscope emitted three flashes during that time interval. Distance between first position and third position was 8.8 cm (3.46 in.).

$$\text{Time taken for three flashes} = \frac{3}{250} = 0.012 \text{ sec.}$$

$$\text{Rebound Velocity} = \frac{\text{Distance}}{\text{Time}} = \frac{8.8}{0.012 \times 100} = 7.3 \text{ m/sec.}$$

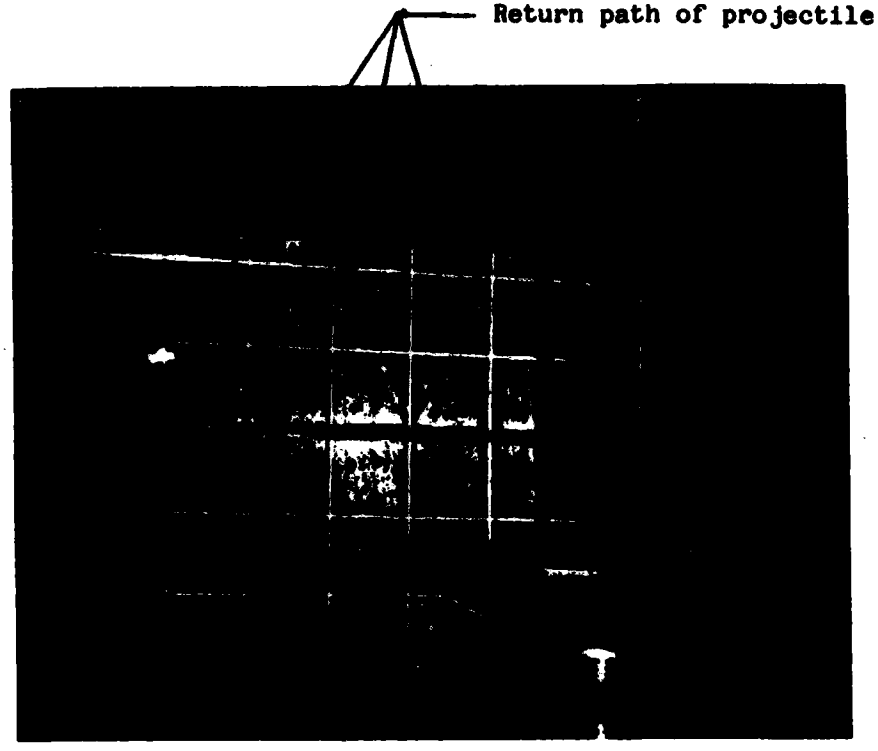

Figure 21. Photograph showing rebound path of projectile after impact.

APPENDIX D

Calculation of Mean Stress Ratio and Standard Deviation of Mean:

Following sample calculation is made for the case of Tension test with no pre-load. Experimental data is taken from Table IV.

Sl. No.	σ_r (x)	$(x - \bar{x})^2$
1	381.2	615.04
2	349.7	44.89
3	351.3	26.01
4	324.4	1024.00
5	390.2	1142.44
6	367.6	125.44
7	412.0	3091.36
8	394.7	1466.89
9	352.6	14.44
10	276.6	6368.04
11	329.4	748.57
12	346.9	90.25
Sum	4276.6	14757.37

Mean σ_r: $\bar{x} = \frac{\text{Sum}}{n} = \frac{4276.6}{12} = 356.4$

Standard deviation: $\sigma = \sqrt{\frac{\Sigma(x-\bar{x})^2}{n-1}} = \sqrt{\frac{14757.4}{11}} = 36.6$

Standard deviation of mean: $\bar{\sigma}_x = \frac{\sigma}{\sqrt{n}} = \frac{36.6}{\sqrt{12}} = 10.6.$

$$\text{Residual Stress} = \begin{cases} 356.4 + 10.6 = 367.0 \text{ GPa} \\ 356.4 - 10.6 = 345.8 \text{ GPa} \end{cases}$$

$$\text{Residual Stress Ratio} = \begin{cases} \frac{367}{398.2} = 0.92 \\ \frac{345.8}{398.2} = 0.88 \end{cases}$$

$$\text{Mean Stress Ratio} = \frac{\bar{x}}{\sigma_o} = \frac{356.4}{398.2} = 0.90$$